Volume 108
Number 2
Summer 2022

Journal of the WASHINGTON ACADEMY OF SCIENCES

ISSN 0043-0439 **Issued Quarterly at Washington DC**

Journal of the Washington Academy of Sciences (ISSN 0043-0439)

Published by the Washington Academy of Sciences
email: editor@washacadsci.org
website: www.washacadsci.org

The Journal of the Washington Academy of Sciences

The *Journal* is the official organ of the Academy. It publishes articles on science policy, the history of science, critical reviews, original science research, proceedings of scholarly meetings of its Affiliated Societies, and other items of interest to its members. It is published quarterly. The last issue of the year contains a directory of the current membership of the Academy.

Subscription Rates

Members, fellows, and life members in good standing receive the Journal free of charge. Subscriptions are available on a calendar year basis, payable in advance. Payment must be made in US currency at the following rates.

US and Canada	$30.00
Other Countries	$35.00
Single Copies (when available)	$15.00

Claims for Missing Issues

Claims must be received within 65 days of mailing. Claims will not be allowed if non-delivery was the result of failure to notify the Academy of a change of address.

Notification of Change of Address

Address changes should be sent promptly to the Academy Office. Notification should contain both old and new addresses and zip codes.

Postmaster:

Send address changes to WAS, Rm 455,
1200 New York Ave. NW
Washington, DC 20005

Academy Office

Washington Academy of Sciences
Room 455
1200 New York Ave. NW
Washington, DC 20005
Phone: (202) 326-8975

Volume 108
Number 2
Summer 2022

Journal of the WASHINGTON ACADEMY OF SCIENCES

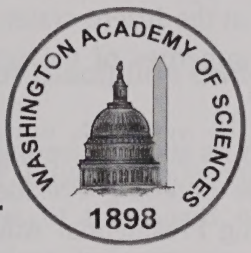

ISSN 0043-0439 **Issued Quarterly at Washington DC**

EDITOR'S COMMENTS

I am pleased to present the 2022 Summer issue of the *Journal of the Washington Academy of Sciences.*

This issue has three papers that once again cover a wide range of science. The first is on a promising non-invasive medical procedure for various psychiatric disorders, especially for depression. The second paper examines photos taken by the most recent Martian rover, *Perseverance*, and makes a convincing argument for a provocative hypothesis for Martian geological processes at the Jezero crater. The third is a fascinating description of the bizarre properties of the supermassive black hole in the center of our galaxy.

The Academy had its annual meeting and awards banquet in May. Ram D. Sriram gave the outgoing Presidential Address, and Lynnette Madsen gave the incoming Presidential Address. Congratulations to the recipients of the 2022 Awards! Their photos and bios are in this issue.

It is with great sadness that we learn of the death of our esteemed colleague and Academy Fellow James Filliben. He received the Award for Distinguished Career in Science in 2017.

Please consider sending in technical papers, review studies, announcements, letters to the editor, comments on papers, suggestions for articles, and ideas for what you would like to see in the Journal to editor@washacadsci.org. Each manuscript is peer reviewed, and there are no page charges.

Kenneth Baclawski

Journal of the Washington Academy of Sciences

Editor Kenneth Baclawski editor@washacadsci.org

Board of Discipline Editors

The *Journal of the Washington Academy of Sciences* has an eleven member Board of Discipline Editors representing many scientific and technical fields. The members of the Board of Discipline Editors are affiliated with a variety of scientific institutions in the Washington area and beyond — government agencies such as the National Institute of Standards and Technology (NIST); universities such as Georgetown; and professional associations such as the Institute of Electrical and Electronics Engineers (IEEE).

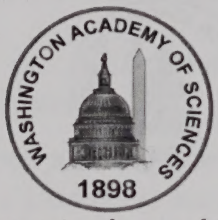

Washington Academy of Sciences
1200 New York Avenue
Rm 455
Washington, DC 20005

Please fill in the blanks and send your application to the address above. We will contact you as soon as your application has been reviewed by the Membership Committee. Thank you for your interest in the Washington Academy of Sciences.

(Dr. Mrs. Mr. Ms)_

_____

Business Address

_____

Home Address

_____

Email

_____

Phone _____

Cell Phone _____

preferred mailing address Type of membership

____Business _____Home ____Regular ____Student

Schools of Higher Education attended	Degrees	Dates

Present Occupation or Professional Position _____
Please list memberships in scientific societies – include office held

_____

_____

Instructions to Authors

1. Deadlines for quarterly submissions are:

Spring – February 1	Fall – August 1
Summer – May 1	Winter – November 1

2. Draft Manuscripts using a word processing program (such as MSWord), not PDF. We do not accept PDF manuscripts.
3. Papers should be 6,000 words or fewer. If there are seven or more graphics, reduce the number of words by 500 for each graphic.
4. Include an abstract of 150-200 words.
5. Use Times New Roman, font size 12.
6. Include two to three sentence bios of the authors.
7. Graphics must be easily resizable by the editor to fit the Journal's page size. Reference the graphic in the text.
8. Use endnotes or footnotes. The bibliography may be in a style considered standard for the discipline or professional field represented by the paper.
9. Submit papers as email attachments to the editor or to editor@washacadsci.org.
10. Include the author's name, affiliation, and contact information - including postal address. Membership in an Academy-affiliated society may also be noted. It is not required.
11. Manuscripts are peer reviewed and become the property of the Washington Academy of Sciences.
12. There are no page charges.

Washington Academy of Sciences
Affiliated Institutions

National Institute for Standards & Technology (NIST)
Meadowlark Botanical Gardens
The John W. Kluge Center of the Library of Congress
Potomac Overlook Regional Park
Koshland Science Museum
American Registry of Pathology
Living Oceans Foundation
National Rural Electric Cooperative Association (NRECA)

Transcranial Magnetic Stimulation

AN ADJUNCTIVE OR POTENTIAL ALTERNATIVE TREATMENT FOR DEPRESSION

Melissa L. Mehalick

Abstract

Transcranial Magnetic Stimulation is a non-invasive treatment for various psychiatric disorders that has been approved by the FDA for treating depression. In this article we explain what this treatment involves and the progress that has been made toward understanding this treatment, both scientifically and clinically, especially for those patients who are suffering from depression and who have not responded to conventional treatments. From the clinical standpoint issues include the safety of the treatment, the length and intensity of treatment, how long the treatment lasts, and the interactions with psychotherapy and medications. Scientifically, the goal is to understand the biological mechanisms that are responsible for the therapeutic effects, especially mechanisms that affect brain regions that regulate mood and cognitive functions.

Introduction

TRANSCRANIAL MAGNETIC STIMULATION (TMS) is a non-invasive form of neuromodulation that has recently been introduced as an adjunctive or alternative method of treatment for various psychiatric disorders. TMS works by placing a magnetic coil against the scalp and delivering weak pulses of electricity. The coil creates an electromagnetic field that is strong enough to stimulate or inhibit the activity of neurons underneath the skull. During the mid-1980s to mid-1990s, TMS was studied primarily in research, and was used as an experimental treatment for depression, but by 2008, the FDA approved an official TMS device for treating depression, particularly for individuals who had not responded well to commonplace treatments such as medications and psychotherapy (Rao, 2018; Perera et al. 2016; Fava, 2003).

Although TMS is a form of brain modulation, it differs greatly from electroconvulsive therapy (ECT), as TMS is given in an outpatient setting, and sedative and/or muscle relaxant medications are not needed for TMS because there is no induction of a seizure. Instead, very mild electrical pulses ranging from approximately 1-50 Hz (though higher

frequencies usually do not exceed 25Hz) are administered while the individual is fully awake. Generally, the lower frequency (<5 Hz) pulses are thought to produce more neural activity inhibition (Chen et al., 1997; Maeda et al., 2000), whereas the higher frequencies (>5 Hz) are thought to produce neural excitation (Maeda et al., 2000; Pascual-Leone et al., 1994). Each individual differs with regard to the amount and level of stimulation needed to achieve therapeutic effects, and differences also depend on the individual's motor threshold, symptom severity, and tolerability.

Clinical Research Studies

Many of the existing clinical research studies examining the effectiveness of TMS have involved studying patients with depression and major depressive disorder (MDD). In general, TMS has been shown to be safe and effective for improving or reducing symptoms of depression. Most of the current research on TMS involves studies where TMS is administered over the dorsolateral prefrontal cortex (DLPFC) for 6-12 weeks for 3-5 sessions per week (O'Reardon et al. 2007). Most of these studies report reductions in depression symptoms in people who receive the active treatment compared to the control group (George et al. 2010; Carpenter et al. 2012). Meta-analyses have found anti-depressive effects when TMS is administered daily (~5 times per week) over the course of 4-6 weeks and given at the site of the prefrontal cortex (Holtzheimer et al. 2001; Burt et al., 2002; Kozel and George, 2002). Some studies have found that TMS treatment is needed for several weeks in order to see robust results or changes in depression symptoms (Polley et al. 2011). For example, McDonald and colleagues found that some individuals needed TMS treatment for 6 weeks (5 days per week of TMS treatment) in order to achieve remission from their depression (McDonald et al. 2011), and another study reported a similar result where depression symptoms were significantly reduced after 28 sessions of TMS (Carpenter et al. 2012).

While TMS appears to be a promising treatment for depression, there remains the question of how long the therapeutic effects last. Cohen and colleagues performed a study where they examined 204 people who received TMS treatment and tracked their depression symptoms for 6 months after receiving TMS. They found that 4 months was approximately the mean time frame to achieve remission, and younger individuals who had received more total TMS sessions tended to have a longer duration of

benefit (Cohen et al. 2009). Another study noted a similar amount of time, where after 109 days (about 3.5 months), 38% of an original sample size of 99 needed a re-introduction or second round of TMS treatment (Janicak et al. 2010). These individuals were not given medications during the first round of TMS treatment, but they were given medications after the completion of TMS, and the investigators reasoned that the individuals who received both the TMS followed by antidepressant medications had the highest success of reaching remission. A third study examined a sample one year after their initial TMS treatment and reported that approximately 60% of the people who had reached remission from depression after TMS, remained in remission a year later. Many of these individuals were also taking antidepressant medications and about 36% received a re-introduction TMS session (average number of sessions was 16) at the one-year point in order to maintain remission. Finally, 45 people did not achieve or maintain remission and 31 of these individuals relapsed within 6 months of receiving the initial round of TMS treatment (Dunner et al. 2014). Taken together, the results of these studies suggest that acute TMS treatment shows efficacy for about 4 months, yet concurrent or follow up treatment with pharmacotherapy and/or undergoing re-introduction TMS sessions on an "as needed" basis appear to facilitate the efficacy of TMS for reaching and maintaining remission.

Re-introduction TMS often occurs several months after the initial TMS treatment and can last anywhere between 3-12 weeks. For some individuals, re-introduction TMS has been helpful, particularly if the frequency and amount of stimulation is adjusted based on the individual's symptoms and mental status over time (Levkovitz et al., 2015; Harel et al., 2014). For individuals who have more severe forms of depression, sometimes a combination of re-introduction TMS, psychotherapy, and medications can be efficacious for reducing symptoms (Wang et al. 2017). In addition to re-introduction TMS, some people with depression benefit from prolonged TMS therapy, which is also known as "maintenance" TMS (Frank et al. 1990; Keller et al., 2007; Klein et al., 2004). Maintenance TMS is given on a reoccurring basis, such as every month, or twice a month, which may occur for as long as 12 months after the initial round of TMS treatment. Maintenance TMS may be a viable option for people who have been chronically depressed and/or who have continuously not responded well to medication and psychotherapy (Philip

et al. 2016). As with re-introduction TMS, maintenance TMS requires some flexibility with altering the frequency and amount of stimulation across time, as well as carefully monitoring symptom changes. Additionally, determining if health insurance companies will cover the cost of maintenance TMS is also important.

Overall, TMS has been shown to be a safe and relatively well-tolerated treatment. The reported side effects of TMS have been very minimal, with the most common being headaches and scalp irritation at the site of coil placement (Janicak et al., 2008). Some of these side effects diminish shortly after treatment and can generally be managed with over-the-counter medications. Other less commonly reported side effects are dizziness, slightly cloudy or impaired cognition, difficulty sleeping, and facial muscle twitches (Janicak et al. 2008). Seizures are a possible but rare side effect of TMS (Dobek et al., 2015), as there have been safety guidelines established for TMS treatment (Rossi et al. 2009). Individuals with epilepsy and/or a history of seizures should carefully consult with their health care providers prior to receiving TMS. Studies offering safety guidelines for preventing seizures during TMS emphasize keeping limits on pulse frequency such that pulses are not given at very close time intervals for a sustained period of time (Chen et al., 1997). One potential reason is that the neurons need time to "recover" or "reset" to their normal resting state before they become stimulated again (Chen et al., 1997).

Scientific Studies

The precise biological mechanisms for how TMS works are still not completely understood, but one hypothesis is that the stimulation acts on AMPA and NMRA receptors to produce mechanisms similar to Long-Term Potentiation (LTP) and Long-Term Depression (LTD), which may facilitate changes in brain function that ultimately lead to the reported therapeutic effects (Nitsche et al. 2003; Funke and Benali, 2011). Given that TMS is often administered over the left DLPFC for management of depression, many studies have examined the physiological changes that occur in this region using fMRI. Generally, studies have reported lower levels of brain activity in the frontal and prefrontal cortex in individuals with depression (Martinot et al. 2011), and after TMS treatment (5-20Hz for 10 sessions), some studies have found increased brain activity, as evidence of increased regional blood flow to the frontal cortex as well as

the limbic system areas (Teneback et al. 1999). Increases in regional blood flow have also been noted in the DLPFC region directly under the coil and in regions more distant to the site of stimulation, including the amygdala, insula, hippocampus, thalamus, and cerebellum (Speer et al. 2000; Nahas et al. 2001). Other studies have reported increased cerebral blood flow to the anterior cingulate cortex (ACC), the orbitofrontal cortex, and putamen, which are also part of the depression neural pathway (Kito et al. 2008; Baeken et al. 2009). In sum, many of the studies described above have found similar results showing that treatment with TMS at the 5-20 Hz range for 10 or more sessions appears to increase blood flow, and hence activity in many of the regions associated with depression.

The Default Mode Network (DMN) is also an important neural network in depression and is responsible for self-referential thought and emotional processing (Mayberg et al. 2000; Greicius et al. 2007). The DMN has many connections among neurons within the prefrontal cortex, the precuneus, and the cingulate cortex (Hagmann et al. 2008), and several studies have found disruptions in the activity and functioning of the DMN (Cooney et al. 2010; Hamilton et al. 2015) in depression. In studies comparing individuals with and without depression, investigators have noted increased activity in the ACC region that appears to influence the overall activity within the DMN (Fox et al. 2012; Fox et al. 2013), as well as increased neuron activity and connectivity within the DMN in individuals with depression (Mayberg et al. 2000; Greicius et al. 2007). When TMS was administered over the left DLPFC in individuals with and without depression, the activity within the ACC was reduced and the activity connections between the ACC and the DMN were also reduced. These results suggest that this effect might be one underlying mechanism of the antidepressant effects of TMS, as one mechanism for depression seems to be altered connectivity between the DMN neural network and in structures such as the ACC that are involved in the brain circuitry underlying depression (Liston et al. 2014; Baeken et a. 2014). Further, activity within the subgenual cingulate has been found to be increased, while activity within the DLPFC has been found to be decreased in people with depression, and activation of these areas with TMS have been found to improve this altered activity and may be another mechanism behind the therapeutic effects of TMS (Fox et al. 2012; Liston et al. 2014). In sum, the above studies offer consistent support that TMS may exert therapeutic

effects by altering or restoring activity to more stable levels in the brain regions that regulate mood and cognitive functions (Nahas et al. 2001 and Teneback et al. 1999).

Conclusion

Progress has been made in the scientific study and clinical use of TMS for treatment and management of depression, as to date, TMS might be a viable option for individuals who have not responded to conventional forms of depression treatment. However, more research is needed to understand the neural mechanisms of action, determine optimal stimulation parameters, and longer-term effects of repeated brain modulation. Nevertheless, TMS remains an interesting topic of study and a ripe area of medicine for incoming and current clinicians to explore.

References

Baeken C, De Raedt R, Van Hove C, et al. 2009. HF-rTMS treatment in medication-resistant melancholic depression: Results from 18FDG-PET brain imaging. *CNS Spectr, 14*(8):439-448.

Baeken C, Marinazzo D, Wu GR, et al. 2014. Accelerated HR-rTMS in treatment-resistant unipolar depression: Insights from subgenual anterior cingulate functional connectivity. *World J Biol Psychiatry, 15*(4):286-297.

Burt T. 2002. Neuropsychiatric applications of transcranial magnetic stimulation: A meta-analysis. Int J *Neuropsychopharmacol, 5*(1):73-103.

Carpenter LL, Janicak PG, Aaronson ST, et al. 2012. Transcranial magnetic stimulation (TMS) for major depression: A multisite, naturalistic, observational study of acute treatment outcomes in clinical practice. *Depress Anxiety, 29*(7):587-596.

Chen R, Classen J, Gerloff C, et al. 1997. Depression of motor cortex excitability by low-frequency transcranial magnetic stimulation. *Neurology, 48*(5):1398-1403.

Cohen RB, Boggio PS, and Fregni F. 2009. Risk factors for relapse after remission with repetitive transcranial magnetic stimulation for the treatment of depression. *Depress Anxiety, 26*(7):682-688.

Cooney RE, Joormann J, Eugene F, et al. 2010. Neural correlates of rumination in depression. *Cog Affect Behave Neurosci, 10*(4):470-478.

Dobek CE, Bumberger DM, Downar J, et al. 2015. Risk seizures in transcranial magnetic stimulation: A clinical review to inform consent process focused on bupropion. *Neuropsychiatr Dis Treat, 11*:2975-2987.

Dunner DL, Aaronson ST, Sackeim HA, et al. 2014. A multisite, naturalistic, observational study of transcranial magnetic stimulation for patients with

pharmacoresistant major depression: Durability of benefit over a 1-year follow up period. *J Clin Psychiatry, 75*(12):1394-1401.

Fava M. 2003. Diagnosis and definition of treatment-resistant depression. *Biol Psychiatry, 58*(8): 649-659.

Fox MD, Buckner RL, White MP, et al. 2012. Efficacy of transcranial magnetic stimulation targets for depression is related to intrinsic functional connectivity with the subgenual cingulate. *Biol Psychiatry, 72*(7):595-603.

Frank E, Kupfer DJ, Perel JM, et al. 1990. Three-year outcomes for maintenance therapies in recurrent depression. *Arch Gen Psychiatry, 47*(12):1093-1099.

Funke K, Benali A. 2011. Modulation of cortical inhibition by rTMS - findings obtained from animal models. *J Physiol*, 589(Pt 18):4423-4435.

George MS, and Belmaker RH. 2007. Transcranial magnetic stimulation in clinical psychiatry. Eds. American Psychiatric Publishing: Arlington, VA.

George MS, Taylor JJ, and Short EB. 2013. The expanding evidence base for rTMS treatment of depression. *Curr Opin Psychiatry, 26*(1): 13-18.

Greicius MD, Flores BH, Menon V, et al. 2007. Resting-state functional connectivity in major depression: abnormally increased contributions from subgenual cingulate cortex and thalamus. *Biol Psychiatry, 62*(5):429-437.

Hagmann P, Cammoun L, Gigandet X, et al. 2008. Mapping the structural core of the human cerebral cortex. *PLos Biol, 6*(7): e159.

Hamilton JP, Farmer M, Fogelman P, et al. 2015. Depression rumination, the default-mode network, and the dark matter of clinical neuroscience. *Biol Psychiatry, 78*(4):224-230.

Harel EV, Rabany L, Deutsch L, et al. 2014. H-Coil repetitive transcranial magnetic stimulation for treatment resistant major depressive disorder: An 18-week continuation safety and feasibility study. *World J of Biol Psychiatry, 15*(4): 298-306.

Holtzheimer PE, McDonald WM, Mufti M, et al. 2010. Accelerated repetitive transcranial magnetic stimulation (aTMS) for treatment-resistant depression. *Depress Anxiety, 27*:960-963.

Janicak PG, Nahas Z, Lisanby SH, et al. 2010. Durability of clinical benefit with transcranial magnetic stimulation (TMS) in treatment of pharmacoresistant major depression: Assessment of relapse during a 6-month, multisite, open-label study. *Brain Stimul, 3*(4):187-199.

Keller MB, Trivedi MH, Thase ME, et al. 2007. The prevention of recurrent episodes of depression with venlafaxine for two years (PREVENT) study: Outcomes from the 2-year and combined maintenance phases. *J Clin Psychiatry, 68*(8): 1246-1256.

Kito S, Fujita K, and Koga Y. 2008. Regional cerebral blood flow changes after low-frequency transcranial magnetic stimulation of the right dorsolateral prefrontal cortex in treatment-resistant depression. *Neuropsychobiology, 58*(1):29-36.

Klein DN, Santiago NJ, Vivian D, et al. 2004. Cognitive-behavioral analysis system of psychotherapy as a maintenance treatment for chronic depression. *J Consult Clin Psychol, 72*(4): 681-688.

Kozel FA, and George MS. 2002. Meta-analysis of left prefrontal repetitive transcranial magnetic stimulation (rTMS) to treat depression. *J Psychiatr Pract, 8*(5):270-275.

Levkovitz Y, Isserles M, Padberg F, et al. 2015. Efficacy and safety of deep transcranial magnetic stimulation for major depression: A prospective multicenter randomized controlled trial. *World Psychiatry, 14*(1): 64-73.

Liston C, Chen AC, Zebley BD, et al. 2014. Default mode network mechanisms of transcranial magnetic stimulation. *Biol Psychiatry, 76*(7):517-526.

Maeda F, Keenan JP, Pascual-Leone A. 2000. Interhemispheric asymmetry of motor cortical excitation in major depression as measured by transcranial magnetic stimulation. *Br J Psychiatry*, 177:169-173.

Mayberg HS, Brannan SK, Tekell JL, et al. 2000. Regional metabolic effects of fluoxetinein major depression: serial changes and relationship to clinical response. *Biol Psychiatry, 48*: 830-843.

McDonald WM, Durkalski V, Ball ER, et al. 2011. Improving the antidepressant efficacy of transcranial magnetic stimulation: Maximizing the number of stimulations and treatment location in treatment-resistant depression. *Depress Anxiety, 28*(11):973-980.

Nahas Z, Teneback CC, Kozel A, et al. 2001. Brain effects of TMS delivered over prefrontal cortex in depressed adults: Role of stimulation frequency and coil-cortex distance. *J Neuropsychiatry Clin Neurosci, 13*(4):459-470.

Nitsche MA, Fricke K, Henschke U, et al. 2003. Pharmacological modulation of cortical excitability shifts induced by transcranial direct current stimulation in humans. *J Physiol*, 553: 293-301.

O'Readon J, Solvason H, Janicak P, et al. 2007. Efficacy and safety of transcranial magnetic stimulation in the acute treatment of major depression: A multisite randomized controlled trial. *Biol Psychiatry, 62*(11):1208-1216.

Paillère Martinot ML, Martinot JL, Ringuenet D, et al. 2011. Baseline brain metabolism in resistant depression and response to transcranial magnetic stimulation. *Neuropsychopharmacology, 36*(13):2710-2719.

Pascual-Leone A, Valls-Sole J, Wassermann EM, et al. 1994. Responses to rapid-rate transcranial magnetic stimulation of the human motor cortex. *Brain, 117*(Pt4):847-858.

Perera T, George MS, Grammer G, et al. 2016. The clinical TMS society consensus review and treatment recommendations for TMS therapy for major depressive disorder. *Brain Stiml*, *9*(3): 336-346.

Philip NS, Dunner DL, Dowd SM, et al. 2016. Can medication free, treatment-resistant, depressed patients who initially respond to TMS be maintained off medications? A prospective, 12-month multisite randomized pilot study. *Brain Stimul*, *9*(2):251-257.

Polley KH, Navarro R, Avery DH, et al. 2011. 2010 Updated Avery-George Holtzheimer Database of rTMS Depression Studies. *Brain Stimul*, *4*(2):115-160.

Rao M. 2018. Transcranial magnetic stimulation. Eds. Bermudes RA, Lanocha KL, and Janicak PG. American Psychological Association Publishing; Arlington, VA.

Speer AM, Kimbrell TA, Wassermann EM, et al. 2000. Opposite effects of high and low frequency rTMS on regional brain activity in depressed patients. *Biol Psychiatry*, *48*(12):1133-1141.

Teneback CC, Nahas Z, Speer AM, et al. 1999. Changes in prefrontal cortex and paralimbic activity in depression following two weeks of daily left prefrontal TMS. *J Neuropsychiatry Clin Neurosci*, *11*(4):426-435.

Wang HN, Wang XX, Zhang RG, et al. 2017. Clustered transcranial magnetic stimulation for the prevention of depressive relapse/recurrence: A randomized controlled trial. *Transl Psychiatry*, *7*(12):1292.

Dr. Melissa Mehalick holds a PhD in Experimental Psychology with concentrations in neuroscience and health psychology. She has worked as a bench scientist studying traumatic brain injury, gut-microbiome and brain interactions, and chronic pain management. She currently works as a portfolio manager for psychological health research, and as a part-time free-lance medical writer.

The Transport of Extrusive Volcanic Deposits on Jezero Crater Through Paleofluvial Processes

Antonio J. Paris and Kate Morgan

Planetary Sciences, Inc.

Abstract

Jezero, an impact crater in the Syrtis Major quadrangle of Mars, is generally thought to have amassed a large body of liquid water in its ancient past. NASA spectra of the proposed paleolake interprets the youngest surface unit as olivine-bearing minerals crystallized from magma. In early 2021, the *Perseverance* rover landed at the leading edge of a fan-delta deposit northwest of Jezero – an area argued to have experienced two distinct periods of fluvial activity. Surface imagery obtained by *Perseverance* reveals partially buried and unburied vesicular and non-vesicular rocks that appear volcanic in origin, emplaced sometime during the Noachian–Hesperian boundary. The absence of volcanic extrusive features along the fan-delta deposit, however, has made the origin of these ballast-like deposits a matter of contention among planetary scientists. To establish the origin of these basalt-like rocks, a comparison was made between analogous deposits on the Moenkopi Plateau in Arizona with similar deposits imaged by *Perseverance* on Jezero. The search for geologic analogs along the Moenkopi Plateau were due to similarities in surface geomorphology, influenced and modified by fluvial, eolian, and past volcanic activity, primarily from the Late Pleistocene-Holocene boundary. By analyzing surface imagery taken by *Perseverance* and paralleling it with the in-situ investigation, we hypothesize that the exposed vesicular rocks imaged by *Perseverance* could have been transported into the paleolake by geomorphic interactions, specifically through fluvial processes – similarly to the basalt deposits that were transported along drainage patterns observed on the Moenkopi Plateau.

Introduction

Jezero Crater is located at latitude 18.38˚N and longitude 77.58˚E in the Syrtis Major quadrangle of Mars (United States Geological Survey, n.d.). The impact crater has a diameter of approximately 49 kilometers and was formed in the late- to mid-Noachian ~4 Gya (NASA, 2020b). Several studies propose the crater was once flooded with liquid water, being home to an ancient river delta, and has undergone significant periods of fluvial and lacustrine activity (Zastrow & Glotch, 2021). Orbital imagery obtained by NASA's High Resolution Imaging Science Experiment

(HiRISE) suggests valley incisions from the paleo-river Neretva Vallis flooded Jezero from the northwest, forming a fan-delta deposit along the crater's rim (Figure 1) (Brown, et al., 2020). Although several studies of the area have concluded that two distinct periods of aqueous activity occurred within Jezero, an analysis of impact craters along inflowing valley networks strongly suggests that the region ceased fluvial activity by the Noachian-Hesperian boundary (Fassett, 2008).

Syrtis Major, an early Hesperian, low relief shield volcano, sits to the south of Jezero. Ancient lava floods from Syrtis Major onlap the southern Noachian exposures of the Nili Fossae, the rim of the Isidis Basin, and many of the ancient fluvial networks along the Syrtis Major quadrangle adjacent to Jezero (Hiesinger & Head, 2004). A recent study proposed that large scale paleo-glaciers could have stopped lava flow from the volcano, which then diverted a network of fluvial systems draining into the Isidis Basin, including Jezero (Matherne, 2019).

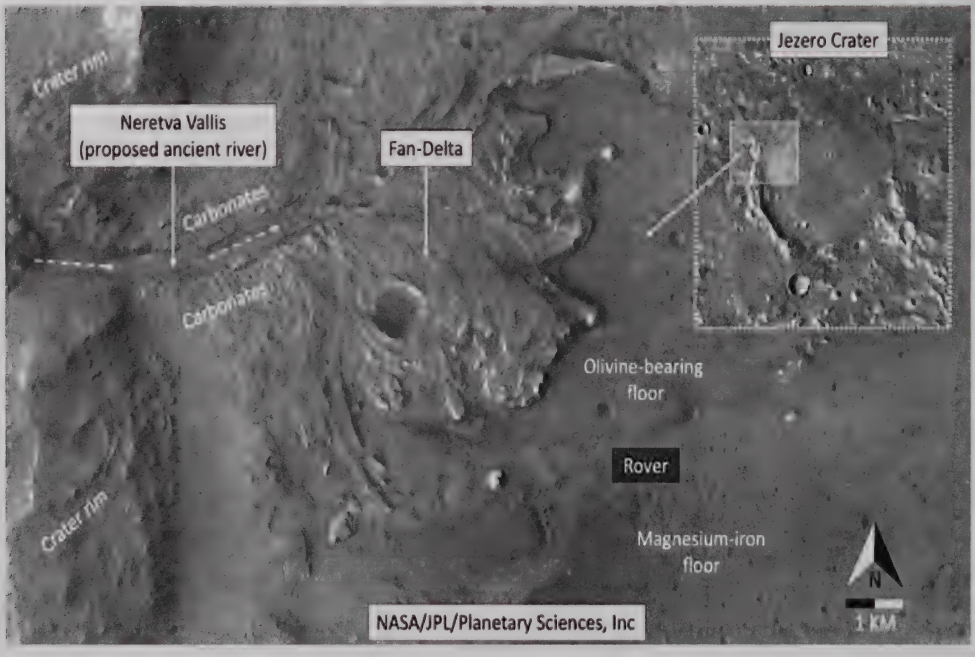

Figure 1: NASA HiRISE image of Jezero Crater and the proposed fan-delta east of the paleo-river Neretva Vallis.

Data Collection

HiRISE and Context Camera (CTX)

The NASA HiRISE and CTX imagery used in this investigation were available through NASA's Planetary Data System (PDS) and the University of Arizona's Lunar and Planetary Laboratory. The datasets used were Mars 2020 Mission 1 (released on 20 Aug 2020) and Mars 2020 Mission 2 (released on 22 Nov 2021). Both cameras are part of the Mars Reconnaissance Orbiter (MRO) currently orbiting Mars. HiRISE can view the surface of Mars with a high-resolution capability, up to ~30 centimeters per pixel, while the CTX camera can observe at ~6 meters per pixel (University of Arizona, n.d.). The MRO also observes the Martian surface earlier in the day; thus, more geomorphic features are evident with partially sunlit floors (Walden et al., 1998).

Mastcam-Z (Left and Right) and Hazard Avoidance Cameras (HazCams)

The surface imagery of Jezero used in this investigation was taken by Mastcam-Z and HazCams. The Mastcam-Z cameras are a multispectral, stereoscopic imaging instrument onboard the *Perseverance* rover. Mastcam-Z consists of two zoom cameras mounted on the remote sensing mast of the rover. The camera has a 3.6:1 zoom capable of broadband red/green/blue imaging and narrow-band visible/near-infrared color imaging. The sensor consists of an ON-Semiconductor KAI-2020CM CCD with an array size of 1600 x 1200 pixels and can image fields of view from 5° to 15° (NASA, 2020a). The HazCams, on the other hand, detect potential hazards in the front and rear pathways of the rover, including large rocks, trenches, and sand dunes. The Hazcams acquire color stereo images of the surface with a field of view from 136° to 102° at 0.46 mrad/pixel. Images taken by *Perseverance* have been made available through NASA's Jet Propulsion Laboratory.

Thermal Emission Spectrometer (TES)

The TES, one of five instruments on the Mars Global Surveyor spacecraft, collects two types of data: hyperspectral thermal infrared data from 6 to 50 μm, and bolometric visible-NIR at 0.3 to 2.9 μm (NASA,

n.d.b). The TES instrument uses the natural harmonic vibrations of the chemical bonds in materials to determine the composition of gases, liquids, and solids on the surface of Mars. TES data used in this investigation were accessed through the Spectral Library at Arizona State University (ASU) and NASA's PDS. These datasets contain calibrated thermal IR radiance spectra, and atmospheric and surface properties.

Compact Reconnaissance Imaging Spectrometer for Mars

CRISM is a visible-infrared spectrometer aboard the MRO and was accessed through the Java Mission-planning and Analysis for Remote Sensing (JMARS). The database is a geospatial information system developed by ASU's Mars Space Flight Facility to provide mission planning and data analysis tools to NASA scientists and instrument team members. CRISM maps the presence of minerals and chemicals, such as iron and oxides, which can be chemically altered by water, as well as phyllosilicates and carbonates, which both form in the presence of water. CRISM measures visible and infrared electromagnetic radiation from 370 to 3920 nanometers (nm) with a spectral sampling of 6.55 nm/channel (NASA, n.d.a). For this investigation, datasets from CRISM's Multispectral Reduced Data Records were analyzed. These consisted of several or more strips of multispectral survey data mosaicked into a map tile (Murchie, 2006). CRISM spectra takes input data in units of I/F (also known as RADF, or Radiance Factor), allowing most reflectance and albedo quantities to be "unitless" quantities (University of Arizona, 2022).

U.S. Geological Survey (USGS)

The geological data used throughout this investigation was obtained from the USGS. Scholarly sources of information focused on the geologic history of Mars and Arizona, while indices in the National Geologic Map Database (NGMDB), e.g., a remote sensing inventory of the Jezero Crater and the Moenkopi Plateau, provided supplementary data. The geologic maps and data in the NGMDB have been standardized in accordance with the Geologic Mapping Act of 1992, section 31f(b), thus meeting widely accepted standards. Data obtained from the U.S. Geological Survey Earth Explorer imagery interface for high altitude aerial imagery also provided a remote sensing inventory of the Moenkopi Plateau.

Autel Robotics Unmanned Aerial Vehicle

The MRO images (HiRISE and CTX) in this investigation were compared with imagery obtained using a crewless aerial vehicle (UAV) operated by Planetary Science, Inc. in situ on the Moenkopi Plateau. The UAV offered a powerful camera on a 3-axis stabilized gimbal that recorded video at 4k resolution up to 60 frames per second. It featured real-glass optics that captured aerial imagery at 12 megapixels from an altitude up to 800 meters and a range of 7 kilometers (Autel Robotics, n.d.).

The Origin of Basalt Deposits on Jezero

Spectra obtained by NASA's CRISM has characterized the surface mineralogy of Jezero and the proposed nearby ancient watershed as an olivine-bearing floor (Sun & Stack, 2020). Olivine is the common name for a suite of iron-magnesium silicate minerals found in many mafic igneous rocks that crystallize from magma and are generally found in the presence of water (Martel, 2003). The transportation of olivine and other basalt deposits into the Jezero by fluvial activity, though, remains a matter of contention. One hypothesis proposes the placement of an olivine-bearing lithology through resurfacing mechanisms ~3.82 Gya during the formation of the Isidis Basin and megabreccia in the Nili Fossae regional basement unit (Mustard et al., 2009).

The abundance of olivine on the crater floor of Jezero, however, is not consistent. Index checks of CRISM, for illustration, assigned a value of 0.00930 (unitless) for olivine on the northwestern rim of the crater, whereas a value of 0.00090 (unitless) is assigned along the east - a differentiation of approximately 164%. Moreover, by superimposing a USGS/CTX mosaic of Jezero (ESP_042315_1985) with the CRISM map tile, the composite noticeably depicts more olivine adjacent to the valley incisions of Neretva Vallis – inferring the deposition of olivine into Jezero was likely through paleo-fluvial processes (Figure 2).

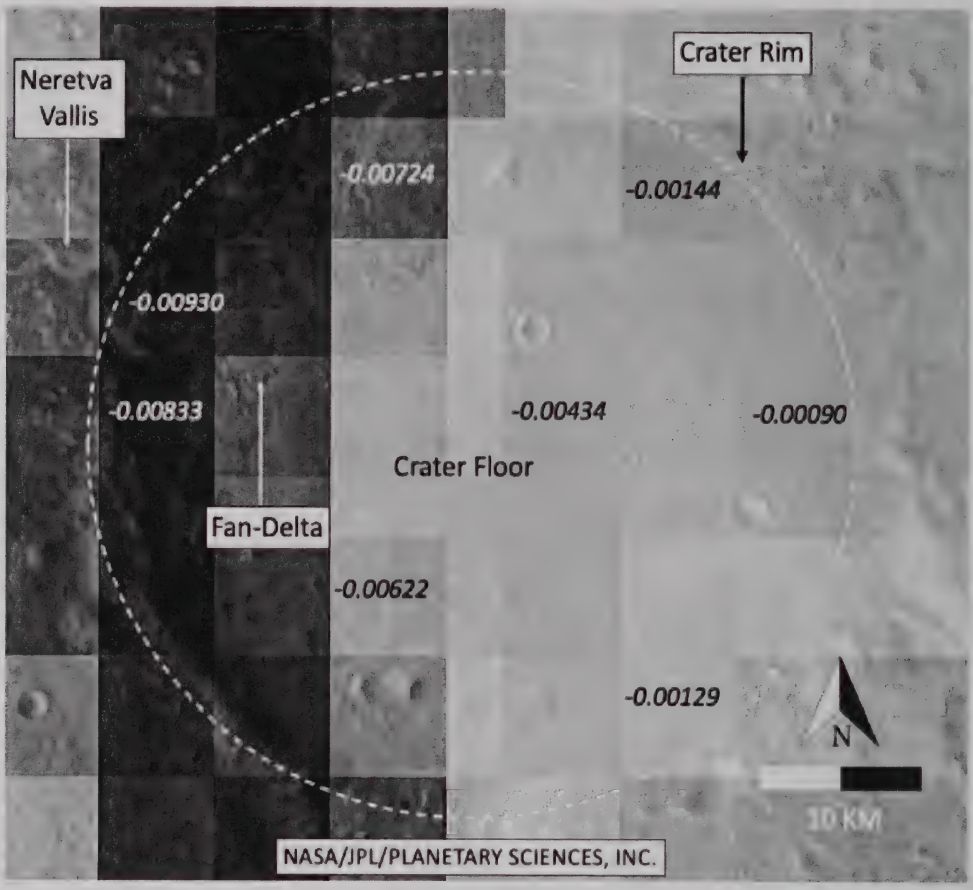

Figure 2: A composite of NASA HiRISE image of Jezero Crater and the NASA CRISM map tile with assigned olivine values.

Another hypothesis suggests that volcanic extrusions during emplacement of the Hesperian ridged plains, or a peak volcanic flux centered in the early Hesperian (which postdates the period of fluvial activity mentioned above), are responsible for ballast deposits inside the paleolakes in this quadrangle (Goldspiel & Squyres, 1991). NASA spectra (TES) of Jezero, however, suggests that flood basalts more than likely were transported by fluvial processes from the highlands, through Neretva Valles, and downslope into the crater. Like the CRISM observations mentioned above, the TES map tile, superimposed over the USGS/CTX image of Jezero, indicates that the occurrence of basalt is greater in the northwest (51.3%) when compared to the occurrence of basalt on the eastern crater floor (21.4%) (Figure 3).

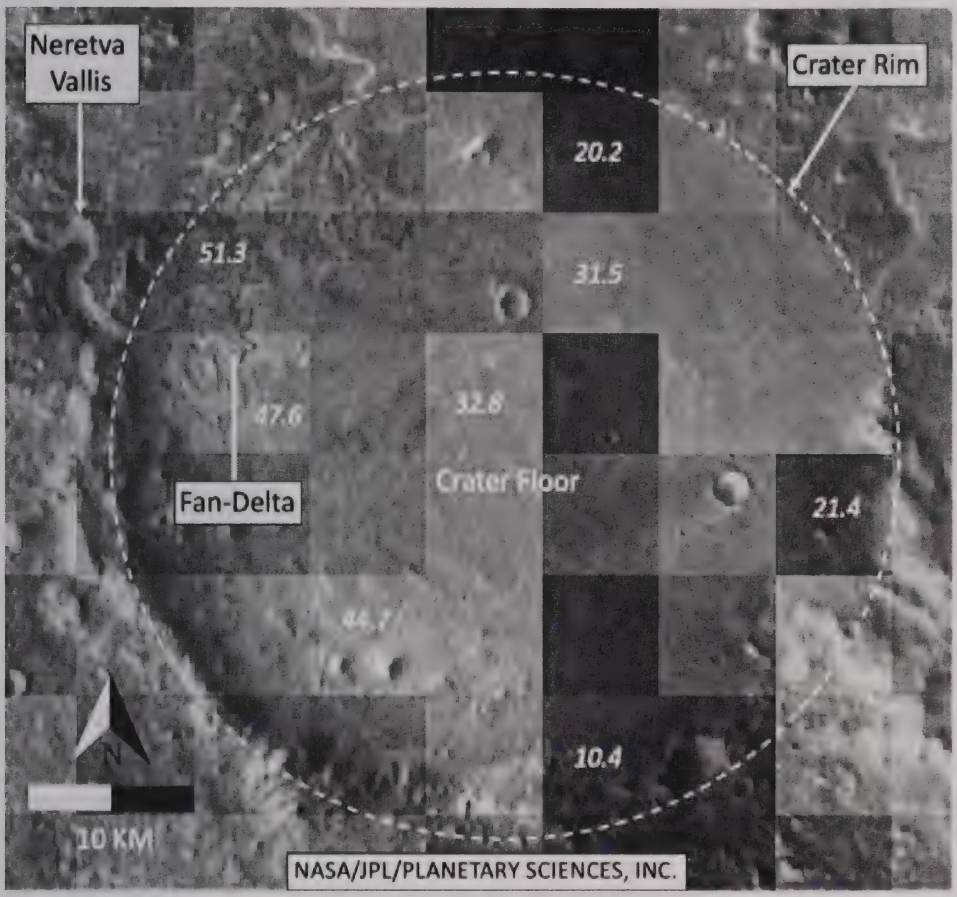

Figure 3: A composite of NASA HiRISE image of Jezero Crater and the NASA TES map tile with assigned basalt values.

Earth Analog: The Moenkopi Plateau and the San Francisco Volcanic Field

This investigation compares volcanic deposits on Jezero Crater with similar geomorphic interactions on the Moenkopi Plateau and the San Francisco Volcanic Field in northern Arizona. We chose the Plateau due to its geologic similarity to Jezero Crater. Specifically, the Moenkopi Plateau consists of various paleo-rivers and alluvial fans in the vicinity of abundant ancient cinder cones – a setting analogous to the paleo-river Neretva Vallis and the proposed fan-delta near the ancient volcano Syrtis Major, both neighboring Jezero. Moreover, the Moenkopi Plateau has been used extensively by NASA as a Martian analog for a range of investigations, to include recent performance testing of the Curiosity

Rover and the Perseverance Rover (Wiens et al., 2021) – an appropriate in-situ setting for this investigation.

The Moenkopi Plateau extends from the Little Colorado River northeastward to the summit, covering 484 kilometers, with elevations ranging from 1,280 meters at the Little Colorado River to 1,700 meters on the plateau (Paris & Tognetti, 2020). The Adeii Eechii Cliffs, an erosional scarp, demarcates the southwest edge of the Moenkopi Plateau. Other major erosional scarps to the southwest include the Red Rock Cliffs and Ward Terrace (Billingsley, 1987b). Nearby, the San Francisco Volcanic Field covers approximately 2,900 kilometers, and during its ~6 Mya history has produced more than 600 volcanoes, most of which are basalt cinder cones (Priest et al., 2001).

Fluvial and eolian deposits in the analog area are dated as Holocene and Pleistocene, undivided (Billingsley, 1987a). Geologically, the plateau consists of exposed sedimentary rocks and volcanic basalt deposits, with surficial deposits consisting of sand dunes, sand sheets, and landside deposits. Sedimentary rocks that consist of silica-cemented sandstone, interbedded limestone, and multi-colored shale plunge to the northeast and form northwest-trending ledges and cliffs. The bedrock in the area of study has been eroded by streams, winds, and a copious supply of loose sediment available for redeposition.

Geomorphic interactions between eolian and fluvial processes since the late Pleistocene are reflected by drainage patterns on northeasterly plunging sedimentary rocks and by the northeastward withdrawal of cuestas along the southwest boundary of the plateau. Tributary drainages, such as the Five Mile, Landmark, Tonahakaaad, Tohachi and Gold Spring Wash, flow southwestward from the edge of the plateau toward the Little Colorado River (Figure 4). These washes, analogous to the fan-delta located on the northwestern rim of Jezero, originate in highland regions along plateaus and tend to form with a rapid change in slope from a high to a low gradient (National Geographic, n.d.). During fluvial activity, the washes transport unconsolidated sediment and rocks at a relatively high velocity due to the steep slope, leaving partially buried and unburied deposits along the leading edge of the wash (Figure 5).

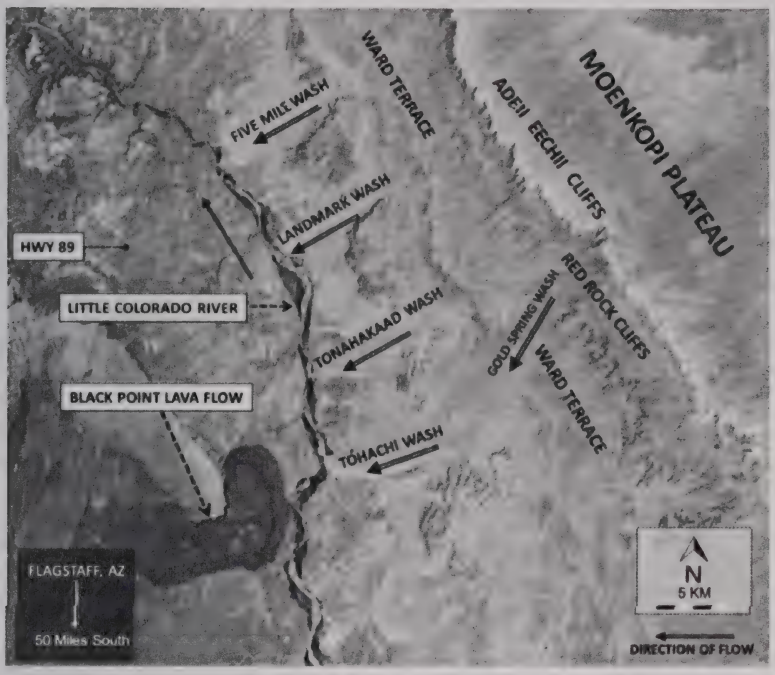

Figure 4: USGS map of the Moenkopi Plateau

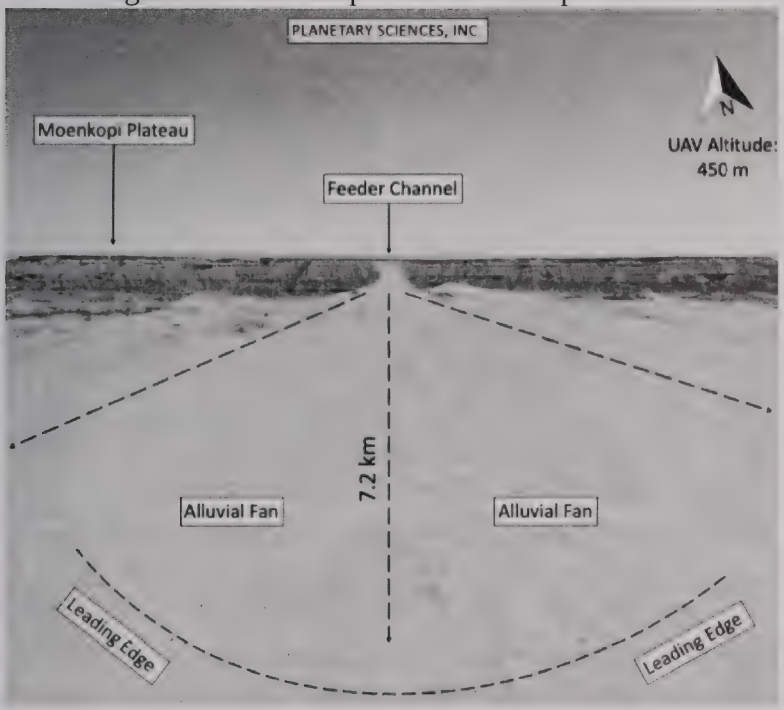

Figure 5: Alluvial fan, analogous to a fan-delta, located on the Moenkopi Plateau (image taken by Planetary Sciences, Inc UAV)

Extrusive Basalt Deposit Analogs

Volcanic activity has played an extensive role in the geologic development of both Earth and Mars. Many of the same magmatic processes have occurred on both planets, leading to sufficiently comparable compositions, and with similar names applied to their igneous rocks, e.g., basalt (Green & Short, 1971). Basalt, for illustration, is a volcanic rock dark in color (generally dark brown, black, or purplish red) (King, n.d.). These rocks are somewhat low in density due to their numerous macroscopic ellipsoidal vesicles (holes) that formed when dissolved gases in the magma come out of solution as it erupts, forming bubbles in the molten rock, some of which remain in place as the rock cools and solidifies (Tietz & Büchner, 2018). Mafic basalt may form as part of a lava flow, typically near its surface, or as fragmental ejecta and generally consist of pyroxene and calcium-rich plagioclase feldspar. Cinder or scoria cones, such as those on the Moenkopi Plateau and the San Francisco Peaks, violently expel lava with high gas content, and due to the vapor bubbles in this mafic lava, the extrusive basalt is formed (University of Saskatchewan, n.d).

In the following section, a sampling of Mastcam-Z and HazCam imagery of basalt-like deposits are exhibited alongside known volcaniclastic deposits unearthed on the Moenkopi Plateau (Holocene to middle Pliocene). The samples, which were photographed in-situ, were chosen because they were found on the leading edge of a fan-like topography, which is analogous to the fan-delta on Jezero. For the purposes of this investigation, sampling was narrowed to specific analogs of basalt: non-vesicular, vesicular, and scoria. As a reference, the analogs on the Moenkopi Plateau were photographed alongside a field ruler with a 10-centimeter arrow facing north.

Analog 1: Extrusive Basalt, Aphanitic, Non-Vesicular

A mafic-like specimen on Jezero Crater was captured by Mastcam-Z (left) on Sol 86 (Figure 6a). These rocks, comparable to our analog (Figure 6b), consist of fine-grained texture with crystals too small to see with the unaided eye, have relatively low silica content and are rich in iron and magnesium. The cooling rate was rapid as heat exchanged with the atmosphere, resulting in few or no vesicles.

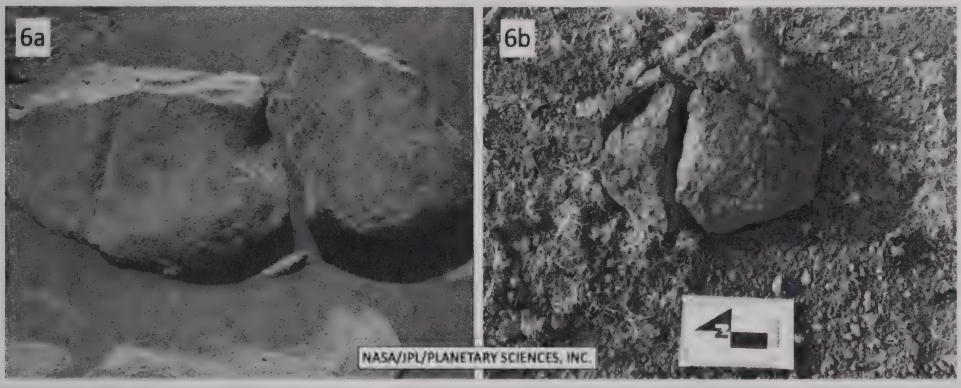

Figure 6: A comparison of Extrusive Basalt, Aphanitic, Non-Vesicular on Jezero Crater (6a) and the Moenkopi Plateau (6b)

Analog 2: Extrusive Basalt, Aphanitic, Vesicular

This specimen on Jezero Crater was taken by Mastcam-Z (left) on Sol 241 (Figure 7a). This vesicular rock is comparable to the analog on the Moenkopi Plateau (Figure 7b). Basalt often shows textural features, such as vesicles, which are formed by the expansion of bubbles of gas or steam during the solidification of the rock.

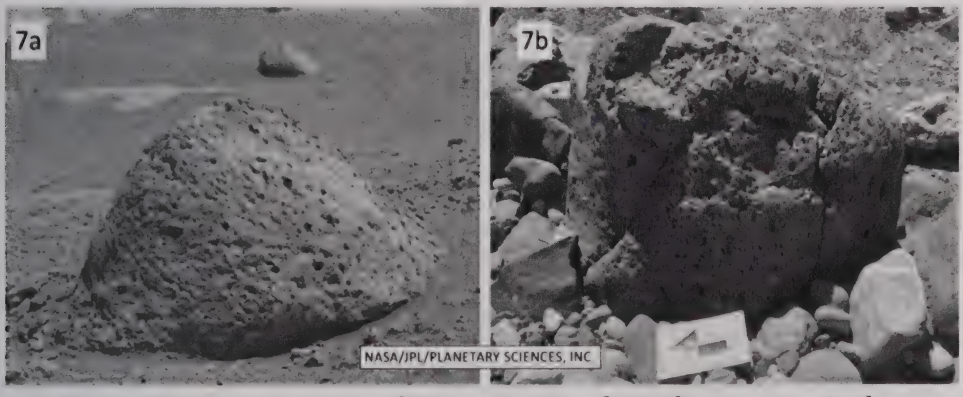

Figure 7: A comparison of Extrusive Basalt, Aphanitic, Vesicular on Jezero Crater (7a) and the Moenkopi Plateau (7b)

Analog 3: Extrusive Basalt, Aphanitic, Highly Vesicular (Scoria)

This specimen on Jezero Crater was photographed by HazCam (right) on Sol 2 (Figure 8a). Scoria, a highly vesicular type of basalt, is common along alluvial fans and washes on the Moenkopi Plateau (Figure 8b). Specimens with a rounded shape, such as these two samples, have

usually been transported by fluvial processes, e.g., rivers and streams (United States Geological Survey, 2013).

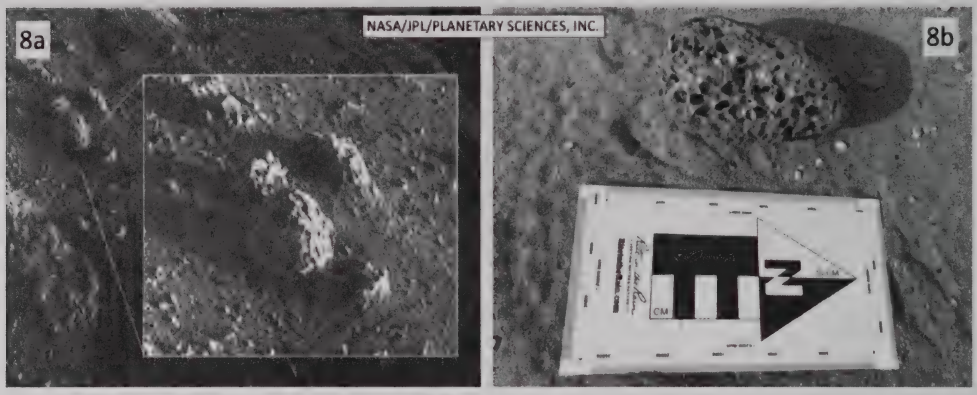

Figure 8: A comparison of Extrusive Basalt, Aphanitic, Scoria on Jezero Crater (8a) and the Moenkopi Plateau (8b)

Analog 4: Extrusive Basalt, Aphanitic, Non-Vesicular, Aeolian Erosion

This image of a mafic-like specimen on Jezero Crater was captured by Mastcam-Z (left) on Sol 183 (Figure 9a). This specimen, however, was sandblasted by Martian winds for eons, a process known as aeolian abrasion. On the Moenkopi Plateau, likewise, winds accelerate to high

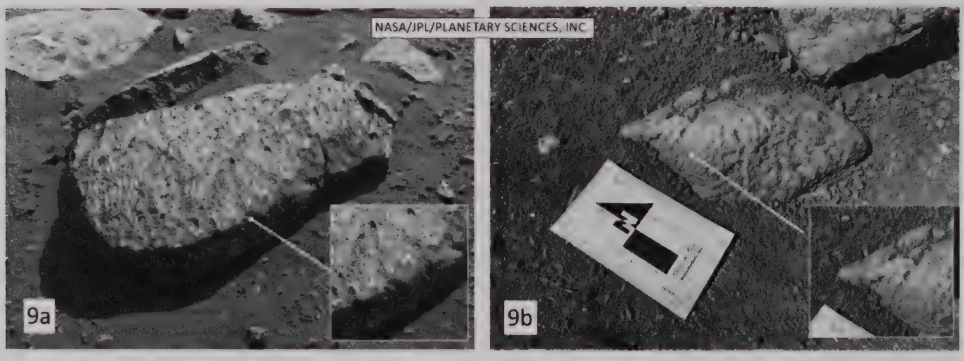

Figure 9: A comparison of Wind Eroded Extrusive Basalt on Jezero Crater (9a) and the Moenkopi Plateau (9b)

speeds so that sand grains impact on rocks. This type of "eon" sandblasting was also evident on numerous basalt specimens along the plateau (Figure 9b).

Analog 5: Extrusive Basalt, Aphanitic, Non-Vesicular, Fractured

This specimen on Jezero Crater was taken by Mastcam-Z (left) on Sol 99 (Figure 10a), which is comparable to the analog on the Moenkopi Plateau (Figure 10b). There are two competing hypotheses for the formation of cracks on Martian rocks. When the paleolake on Jezero dried up, the basalt rock slowly cracked apart under the weak Martian Sun. Alternatively, ancient weathering on Mars provided conditions for frequent freeze/thaw cycles that produced ice wedging – a type of mechanical weathering found on Earth that breaks apart using the expansion of freezing water.

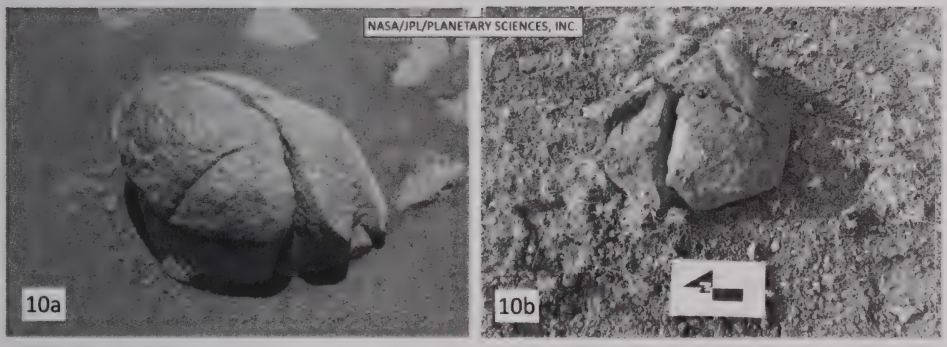

Figure 10: A comparison of Fractured Extrusive Basalt on Jezero Crater (10a) and the Moenkopi Plateau (10b)

Interpretation and Conclusion

A comparison of the images taken by the *Perseverance* and the Moenkopi analogs infer comparable basaltic deposits. NASA spectra of CRISM and TES, moreover, revealed an abundance of flood basalts along the leading edge of the fan-delta (51.3%) when compared to the crater floor on the east (21.4%). We hypothesize, therefore, that the deposits were more than likely emplaced during the Late Noachian, conceivably in multiple, localized episodes of redeposition. During this time, deposits of flood basalts from the volcano Syrtis Major were transported east and downslope from the highlands by water, glaciation, or both along the deltas and other fluvial networks, such as the valley incisions of Neretva Vallis, into the proposed paleo-basin (Figure 9). After the cessation of open water, partially buried and unburied basalt deposits became exposed, predominantly by post eolian activity. These geomorphic interactions on

Jezero, specifically the paleo-fluvial processes mentioned above, are consistent with the basalt that was transported and redeposited along drainage patterns observed on the Moenkopi Plateau.

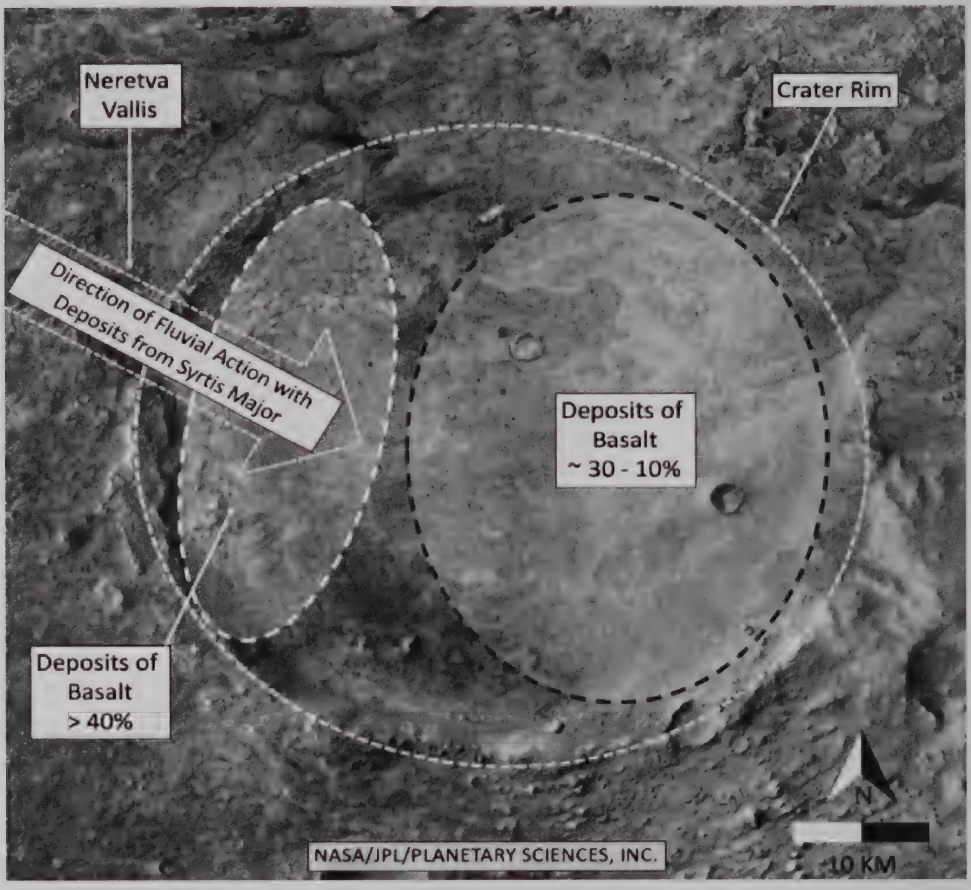

Figure 9: The transport of basalt deposits into Jezero Crater

References

Autel Robotics. (n.d.). *EVO series*. auteldrones.com. https://bit.ly/3wMIB3d

Billingsley, G. H. (1987a). *Geologic map of the southwestern Moenkopi Plateau and southern Ward Terrace, Coconino County, Arizona [The Landmark, Gold Spring, Wupatki NE, Badger Spring, and Rock Head 7.5 min]*. [Map]. U.S. Geological Survey. https://bit.ly/39OvUNw

Billingsley, G. H. (1987b). *Geology and geomorphology of the southwestern Moenkopi Plateau and southern Ward Terrace, Arizona*. U.S. Geological Survey. https://pubs.usgs.gov/bul/1672/report.pdf

Brown A. J., Viviano, C. E., & Goudge, T. A. (2020). Olivine-carbonate mineralogy of Jezero Crater. *Journal of Geophysical Research: Planets*, *125*(3), 1–30. https://doi.org/10.1029/2019JE006011

Fassett, C. I. (2008). Valley network-fed, open-basin lakes on Mars: Distribution and implications for Noachian surface and subsurface hydrology. *Icarus*, *198*(1), 37–56. https://doi.org/10.1016/j.icarus.2008.06.016

Goldspiel, J. M., & Squyres, S. W. (1991). Ancient aqueous sedimentation on Mars. *Icarus*, *89*(2), 392–410. https://doi.org/10.1016/0019-1035(91)90186-W

Green, S., & Short, N. M. (Eds.). (1971). *Volcanic landforms and surface features: A photographic atlas and glossary*. Springer.

Hiesinger, H., & Head, J. W. (2004). The Syrtis Major volcanic province, Mars: Synthesis from Mars Global Surveyor data. *Journal of Geophysical Research*, *109*(E01004), 1–37. https://doi.org/10.1029/2003JE002143

King, H. (n.d.). *Scoria*. Geology.com. https://geology.com/rocks/scoria.shtml

Martel, L. M. V. (2003, November 3). *Pretty green mineral--Pretty dry Mars?* Planetary Science Research Discoveries. http://www.psrd.hawaii.edu/Nov03/olivine.html

Matherne, C. M. (2019). *Role of glaciers in halting Syrtis Major lava flows to preserve and divert a fluvial system*. [Unpublished master's thesis]. Louisiana State University. https://bit.ly/3PH1Sfh

Murchie, S. (2006). *Mars Reconnaissance Orbiter Compact Reconnaissance Imaging Spectrometer for Mars Multispectral Reduced Data Record, MRO-M-CRISM-5-RDR-*

MULTISPECTRAL-V1.0. NASA Planetary Data System. https://bit.ly/3PCO3yn

Mustard, J. F., Ehlmann, B. L., Murchie, S. L., Poulet, F., Mangold, N., Head, J. W., Bibring, J., & Roach, L. H. (2009). Composition, morphology, and stratigraphy of Noachian Crust around the Isidis Basin. *Journal of Geophysical Research*, *114*(2), 1–18. https://doi.org/10.1029/2009JE003349

NASA. (n.d.a). *Compact Reconnaissance Imaging Spectrometer for Mars (CRISM) Fact Sheet*. MARS Reconnaissance Orbiter. https://go.nasa.gov/3PFqWDi

NASA (n.d.b). *The Thermal Emission Spectrometer (TES) fact sheet*. Planetary Data System. https://bit.ly/3wPxmqZ

NASA. (2020a). *Mastcam-Z for scientists*. Mars 2020 Mission: Perseverance Rover. https://go.nasa.gov/3NPQHPJ

NASA. (2020b). *Perseverance rover's landing site: Jezero Crater*. Mars 2020 Mission: Perseverance Rover. https://go.nasa.gov/3a9iYBY

National Geographic Society. (n.d.). *Alluvial fan*. Resource Library, Encyclopedic Entry. https://www.nationalgeographic.org/encyclopedia/alluvial-fan/

Paris, A. J., & Tognetti, L. A. (2020). Ancient river morphological features on Mars versus Arizona's Moenkopi Plateau. *Washington Academy of Sciences, 106*(1), 59–76. https://doi.org/10.48550/arXiv.2005.00349

Priest, S., Duffield, W., Malis-Clark, K., Hendley II, J., & Stauffer, P. (2001, April 16). *The San Francisco Volcanic Field, Arizona*. U.S. Geological Survey Fact Sheet 017-01. https://pubs.usgs.gov/fs/2001/fs017-01/

Sun, V. Z. & Stack, K. M. (2020). *Geologic map of Jezero Crater and the Nili Planum region, Mars*. [Map]. U.S. Geological Survey. https://doi.org/10.3133/sim3464

Tietz, O., & Büchner, J. (2018). The origin of the term 'basalt,' *Journal of Geosciences, 63*(4), 295–298. http://doi.org/10.3190/jgeosci.273

United States Geological Survey. (n.d.). *Map of Jezero Crater on Mars*. Gazetteer of Planetary Nomenclature. https://on.doi.gov/3LWMCrD

United States Geological Survey. (2013). *Scoria*. Volcano Hazards Program. https://volcanoes.usgs.gov/vsc/glossary/scoria.html

University of Arizona. (n.d.). *ABOUT US: Principal & co-investigators*. Lunar & Planetary Laboratory HiRISE. https://www.uahirise.org/epo/about/

University of Arizona. (2022). *Algorithm descriptions and image processing*. UA Campus Repository. https://bit.ly/3wFWHo7

University of Saskatchewan. (n.d.). *Classification of igneous rocks*. Physical Geology. https://bit.ly/38cMG8A

Walden, B. E., Billings, T. L., York, C. L., Gillett, S. L., & Herbert, M. V. (1998). Utility of lava tubes on other worlds. *Lunar and Planetary Institute Report*, 16–17. https://bit.ly/38FVfJv

Wiens, R.C. (2021). The SuperCam Instrument Suite on the NASA Mars 2020 Rover: Body Unit and Combined System Tests. Space Sci Rev 217, 4. https://doi.org/10.1007/s11214-020-00777-5

Zastrow, A. M., & Glotch, T. D. (2021). Distinct carbonate lithologies in Jezero Crater, Mars. *Geophysical Research Letters, 48*, 1–10. https://bit.ly/38O2uPl

ANTONIO PARIS, PH.D., is the Chief Scientist at Planetary Sciences, Inc., a former assistant professor of astrophysics at St. Petersburg College, Florida, and a graduate of the NASA Mars Education Program at the Mars Space Flight Center, Arizona State University. He is the author of *Mars: Your Personal 3D Journey to the Red Planet* and is a professional member of the Washington Academy of Sciences, the American Astronomical Society, and a fellow at the Explorers Club.

KATE MORGAN assisted Planetary Sciences, Inc. in-situ as a research assistant during this investigation. Kate collected, photographed, and made a record of the basalt deposits used for this study. She holds a Bachelor of Science degree in biology and is a recent graduate of Project POSSUM, a NASA-supported program designed to expand on bioastronautics and human factors research, providing a foundation for future space missions.

The Supermassive Black Hole at the Center of the Milky Way

Sethanne Howard

USNO/retired

Abstract

The 2020 Nobel Prize in Physics was for the verification of the supermassive compact object at the center of our Milky Way. The Prize went to three people, one for showing black holes can exist, and two for showing that the supermassive compact object at the center of the Milky Way is compatible with a supermassive black hole. We investigate how black holes can exist, and we study how the team observing the center of the Milky Way concluded that there must be a supermassive black hole there. We discuss the latest image of the Milky Way center.

Introduction

THE IDEA OF BLACK HOLES has been around for a long time. They are thought to be small dark objects with an escape velocity greater than the speed of light. In other words a black hole is an object from which nothing can escape, even light.

Black holes (although they were not called that) were mentioned in the late 18th century. The first scientists to discuss the possibility of dark objects with an escape velocity larger than the speed of light were the English polymath astronomer and priest John Michell in 1783 (Michell, 1784), and the French polymath Pierre-Simon Laplace in works from 1796 and 1799.

Michell's paper had the unwieldy title of: "On the Means of Discovering the Distance, Magnitude, &c. of the Fixed Stars, in Consequence of the Diminution of the Velocity of Their Light, in Case Such a Diminution Should be Found to Take Place in any of Them, and Such Other Data Should be Procured from Observations, as Would be Farther Necessary for That Purpose." See Orchiston (2009) for the details of Michell's work.

LaPlace stated: "The gravitation attraction of a star with a diameter 250 times that of the Sun and comparable in density to the Earth would be

so great no light could escape from its surface. The largest bodies in the universe may thus be invisible by reason of their magnitude." (Orchiston, 2009)

The idea was then ignored until the 20th century. It was not generally believed that the gravitational pull of an object could affect light; however, we still have something interesting to learn. Henry Cavendish in 1784 (in an unpublished manuscript) and Johann Georg von Soldner in 1801 (published in 1804) had pointed out that Newtonian gravity predicts that starlight will bend around a massive object like the Sun. Soldner even calculated the amount that starlight would be bent by the Sun.

According to Newton we have the total energy of an object depending on motion (kinetic) and position (potential):

Energy = Kinetic Energy + Potential Energy.

To investigate the dark object in the Newtonian universe, place a test particle of mass m at the edge of the dark object. Let it move at the speed of light, c, so it can just barely, if at all, escape the dark object. We use modern notation to get Kinetic energy = $\frac{1}{2}mv^2$, where m is the mass of the test particle and v is the velocity of the test particle – in this case, c. The potential energy = $-\frac{GMm}{r}$, where G is the gravitational constant, M is the mass of the dark object, m is the mass of the test particle, and r is the radius of the dark object. Set the total energy of a test particle at the edge of the dark object to zero (in other words the test particle is going nowhere even though it is moving at the speed of light). In that case:

$$\frac{1}{2}mv^2 - \frac{GMm}{r} = 0.$$

Solving this equation for r we get:

$$r = \frac{2GM}{c^2}.$$

Note that if the dark object has a radius less than r, the test particle could only escape if it had a velocity greater than c. As the radius

decreases the escape velocity approaches infinity. This same equation with a different meaning will show up in Einstein's universe.

The Einstein Universe

It took Albert Einstein (and others) to show that gravity can influence light. First with his Special Theory of Relativity and second with his General Theory of Relativity he proved that gravity does influence the motion of light. Einstein postulated that the speed of light, *c*, is the maximum speed that can exist. No object can move faster than *c*. He did that in 1905 when setting forth the Special Theory of Relativity. He published the General Theory of Relativity (GTR) in 1915. He used a four-component space-time with three space components and one time component.

There have been innumerable tests of the GTR. It has yet to fail a test. One of the first such tests occurred during the solar eclipse of May 29, 1919. The starlight matched the predicted amount of bending from GTR and disagreed with the amount calculated by Soldner. The amount predicted by GTR is twice Soldner's amount.

The description of the curvature (warping) of space is the mathematically complicated part of GTR. It involves tensor calculus and metrics. The equations of GTR are a set of sixteen tensor equations expressed as follows:

$$G_{\mu}^{\nu} + \Lambda g_{\mu}^{\nu} = \frac{8\pi G}{c^4} T_{\mu}^{\nu}.$$

In this expression, μ and ν are the indices of the space and time components. Since there are four space-time components, each index has four values, so there are sixteen values for the pair of indices. A tensor is a geometrical higher-order vector. The number of indices needed to represent a tensor is its order. A tensor of order 0 is a scalar, order 1 is a vector, order 2 is a matrix. The tensor G_{μ}^{ν} in the GTR has two indices, so it is a matrix. G_{μ}^{ν} is the Einstein tensor, which represents the curvature in a Riemannian manifold. The scalar Λ is the cosmological constant. Einstein called Λ his greatest blunder. Today scientists use it to explain 'dark energy'. It was originally introduced by Einstein to allow for a static universe (*i.e.*, one that is not expanding or contracting). This effort was

unsuccessful for two reasons: the static universe described by this theory is unstable, and observations of distant galaxies by Hubble a decade later confirmed that our universe is, in fact, not static but expanding. The tensor g_{μ}^{ν} is the gravitational metric tensor. I think of a metric as a flexible, twistable ruler that allows one to measure distances between two events. Finally, T_{μ}^{ν} is the stress-energy tensor. A metric is a solution to the equations of GTR.

The first solution came within a few months. This was during WWI. Karl Schwarzschild published a solution (metric) to the equations of GTR. He sent the solution to Einstein. Then, unfortunately, as a member of the German army he was sent to the Russian front where he fell ill and died. However, his letter reached Einstein. Schwarzschild had produced a metric for a curved space-time around a spherically symmetric non-rotating mass.

See Howard (2011) for a discussion of metrics and how they play with GTR. The Schwarzschild Metric in spherical coordinates is:

$$c^2 d\tau^2 = \left(1 - \frac{2Gm}{c^2 r}\right) c^2 dt^2 - \left(1 - \frac{2Gm}{c^2 r}\right)^{-1} dr^2 - r^3 d\Omega^2$$

By looking at the first term on the right side of the equation we see that at $r = 0$ there is a **singularity** - a place where the laws of science do not apply and cannot be used. At the singularity the term 1/0 is undefined, not zero and not infinity.

The second term on the right side of the equation also contains a situation where r can equal 0. This occurs at $r = \frac{2GM}{c^2}$. This equation became known as the **Schwarzschild radius** or **event horizon**. It is an artificial singularity due to the choice of a spherical coordinate system. The singularity disappears when a different coordinate system is used. Note that this is the same equation as shown above from the 18th century. So what is it? It defines a radius that surrounds the real singularity.

The meanings of the singularity and the Schwarzschild radius were studied for some time. Was it real or was it an artifact? In 1939 two scientists showed that for the spherical case the Schwarzschild radius

represented a horizon such that the object tends to close itself off from communication with distant observers; only its gravitational field persists (cosmic censorship – we are not allowed to see the center) (Oppenheimer and Snyder, 1939). However even Einstein was not happy with the reality of an event horizon.

Then in the late 1950s and through the 1960s a new set of observations appeared: quasi-stellar objects (QSO or quasars) that were far too bright for a normal star or galaxy were observed. Eventually they were called active galactic nuclei (AGN) which exist at large distances from the Milky Way. These objects were seen at redshift $z > 2$ which is a very large redshift. These objects show rapid and random energy variations indicating a small and powerful source of energy. Astronomers eventually realized that quasars were not isolated objects but the extremely luminous centers of distant galaxies.

There is also a class of galaxies known as Seyfert galaxies. These are galaxies with an over-bright center. They are not as distant as quasars. However the over-bright center drove the total mass of the galaxy higher than expected (Private communication) or even believable. These galaxies are now bunched with QSOs, the total group known as AGNs.

AGNs are galaxies, but they are not typical galaxies. Typical galaxies have a luminosity structure that is smooth from end to end. AGNs have a large spike in luminosity at their centers.

Metrics

In the meantime other metrics (solutions to GTR) were derived. All of these metrics assume that the universe is isotopic and homogeneous.

We have the Schwarzschild metric for a spherical non-rotating, uncharged black hole. The corresponding solution for a charged, spherical, non-rotating body, the Reissner-Nordström metric, was discovered soon afterwards. The Kerr metric solves the Einstein equations for an uncharged axially symmetric rotating mass. The corresponding metric for a charged axially symmetric rotating mass is the Kerr-Newman metric. The reader can Google these metrics to find the equations. They are too complicated to include here. The Hartle–Thorne metric is a space-time metric that describes the exterior of a slowly and rigidly rotating,

stationary, and axially symmetric body. It is an approximate solution of the vacuum Einstein equations.

Then there is the Friedmann-Lemaître-Robertson-Walker (FLRW) metric. It describes a homogeneous, isotropic, expanding (or otherwise, contracting) universe that is path-connected, but not necessarily simply connected. It is customarily grouped in sections: The Friedmann metric, the Robertson-Walker metric, or the Friedmann-Lemaître metric. These define the standard model of cosmology. The metrics were developed in the 1920s and 1930s. They formed exact solutions to the Einstein equations.

Lemaître was the first to theorize that the universe is expanding – shortly afterward confirmed by Edwin Hubble's observations of distant galaxies. Lemaître also proposed the "big bang" origin of the universe. Hubble's observations led to Hubble's Law representing the expansion of the universe. Although long known as the Hubble Law, in 2018 the International Astronomical Union voted to honor Lemaître and renamed this the Hubble-Lemaître Law representing the expansion of the universe.

The Singularity Theorem

The discovery of quasars led astronomers to study the gravitational collapse of an object that might lead to a singularity. In other words what could cause such extreme energies? Maybe the collapse created extreme energy.

A critical observable for black holes is the innermost stable circular orbit, which is at a distance three Schwarzschild radii from a Schwarzschild (non-rotating) black hole. Matter closer than that will fall directly into the black hole, adding to its mass. Furthermore, as matter spirals in, up to between 6% and 42% of its rest-mass energy can be released, depending on the rotational energy and the black hole spin direction with respect to the spiraling in-falling matter. This is the source of the energy we observe in x-ray and radio (optical for quasars).

Roger Penrose analyzed the situation without the assumption of spherical symmetry, assuming only that the collapsing matter had a positive energy density. Without spherical symmetry he had to invent new mathematical methods. He introduced the concept of a *trapped surface*. A

trapped surface is a closed two-dimensional surface with the property that all light rays orthogonal to the surface converge at the origin when traced toward the future.

For spherical symmetry any spherical surface with a radius less than the Schwarzschild radius is a trapped surface. The radial direction becomes time-like as one passes through the event horizon. Time and space switch roles at the horizon and the direction inwards, towards the origin of spherical coordinates, becomes time. The flow of time inevitably will bring any observer towards the origin of the radial coordinate, where time ends. There is no option to stop the march to the origin. All the mass that formed the black hole resides at this single moment in time, the singularity.

Such trapped surfaces can also be found in the case of rotating black holes. In fact the trapped surface remains, regardless of how the solution is perturbed, and its existence is independent of any assumptions about symmetry. Penrose then proved that once a trapped surface had formed, it is impossible, within the GTR and with a positive energy density, to prevent the collapse towards a singularity (Penrose, 1965). This concept is the first post-Einstein result in GTR. Once a trapped surface forms, the formation of a black hole is inevitable. The question of the singularity was answered. Given a metric solution a black hole will form. It is for this that Penrose was included in the 2020 Nobel Prize. Black Holes can exist.

Robert Dicke was the first to use the term ‘black hole’ during lectures at Princeton in 1960, and Wheeler later helped make it popular. Even though black holes are neither black nor a hole, the term caught on. Supermassive black holes became candidates for the centers of AGNs. Astronomers followed this by suggesting that most galaxies contain a supermassive black hole at their centers, even the Milky Way.

Masers Enter the Picture

Matter spiraling in to the galaxy center, if a supermassive black hole is there, will produce rapid kinematic motion, spiraling faster and faster as it approaches the center. Astronomers first thought that a dense group of stars could cause this rapid motion. Miyoshi *et al.* (1995) were the first to claim that a dense stellar population could not account for the

rapid motion around a galactic center. They made observations of a rotating water maser disc at 0.13 pc from the center of one of the closest active AGNs, the nucleus of the galaxy NGC 4258 which is at a distance of 7.3 Mpc from us.[1] Observations made at the 1.3-cm radio wavelength Very Long Baseline Array (VLBA) showed a thin disk containing water masers surrounding the mildly active nucleus.

Exploiting the power of the Very Long Baseline Interferometry (VLBI) technique, they mapped the location and velocity of the masers with an angular resolution better than a milliarcsecond. This is remarkably precise, better than the Hubble Space Telescope. The rotation curves follow Keplerian orbits around the compact central source which has a mass of $3.7 \times 10^7 M_{\odot,}$ corresponding to a density in excess of a few $\times 10^9 M_{\odot}\, pc^{-3}$. This density is inconsistent with a long-lived dense cluster of stars. The group announced their results at a press conference at a meeting of the American Astronomical Society. Their technique is independent of the method used to measure the Hubble constant by the Hubble Space Telescope which relied on Cepheid variables. They provide an excellent way to measure the Hubble constant that does not depend upon Cepheid variables.

The Milky Way

The Milky Way is our home galaxy. The solar system revolves about the center taking about 200 million years to complete one trip around the Milky Way. We are about eight kpc from the center[2]. There is a complex radio source at the Milky Way center called Sagittarius A* (Sgr A*). It is so named because it is in the constellation Sagittarius. The center of the Milky Way is obscured by dust which makes it unavailable to optical light. Radio waves, however, can easily penetrate the dust. This is why the central region was first observed in the radio regime. Also certain regions of the infra-red can penetrate the dust but that could not occur until we had large enough telescopes with infra-red detectors.

VLBI observers measured the diameter of this radio source as 44 million km. That sounds like a lot but let us compare it to the solar system.

[1]A parsec is 3.0637 x 10^{16} m or the distance from the Sun to the celestial object at which 1 AU subtends one arcsecond. A kiloparsec (kpc) is 1000 parsecs. A megaparsec (Mpc) is a million parsecs.

The distance of Mercury from the Sun as 46 million km. This is at closest approach. So the diameter of Sgr A* is slightly less than Mercury's distance from the Sun. In other words Sgr A* is a very bright, very compact radio source.

If Sgr A* is a supermassive black hole then the typical speeds of stars in the region should be proportional to $1/\sqrt{r}$ where r is the distance from the center. In other words as r decreases the speed increases. These Keplerian orbits will not occur if Sgr A* is composed of a spatially extended group of stars.

Measuring the Speeds around Sgr A*

Measuring the speeds of the stars around Sgr A* is crucial to checking its black hole status. Are the speeds Keplerian? For nearly three decades two observational teams, one led by Genzel at the Max Planck Institute for Extraterrestrial Physics (MPE) and the other by Ghez at the University of California, Los Angeles (UCLA), have monitored the motions of stars orbiting the Galactic center. Genzel's group used telescopes in Chile operated by the European Southern Observatory (ESO), while Ghez and her colleagues used the Keck 8-meter Observatory in Hawaii. The agreement between the two teams was excellent.

The work cannot be done in the visual range of the spectrum. There is too much dust in the Galactic center that blocks the optical light. So they observed stars in the near-infrared. They used both speckle imaging[2] and adaptive optics[3] to reduce the inherent jitter of stars due to Figure 1. Position of some S stars in 1995. The star represents Sgr A*.the Earth's atmosphere.

They used a set of stars in the Galactic center that they called S stars. Figure 1 shows where the stars were in 1995. Star S2 is especially interesting. It has a very elliptical orbit with a period of 16 years. They were able to obtain a full orbit for this star. See Figure 2 and Figure 3 for the details (courtesy Nobel Prize Committee 2020). Sgr A* is located just inside the orbit of S2 near the bottom of Figure 2.

[2]Take a large number of short images that individually freeze the jitter, and then stack them together.
[3]Deform the telescope mirror in real time to compensate for the jitter of the star.

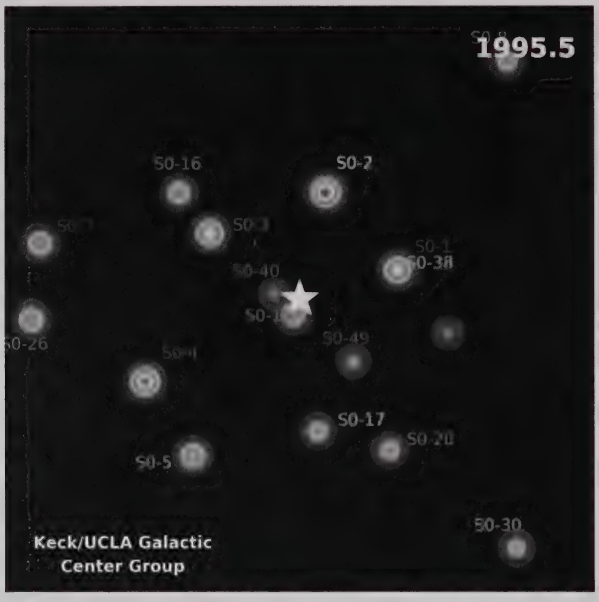

Figure 1. Position of some S stars in 1995. The star represents Sgr A*.

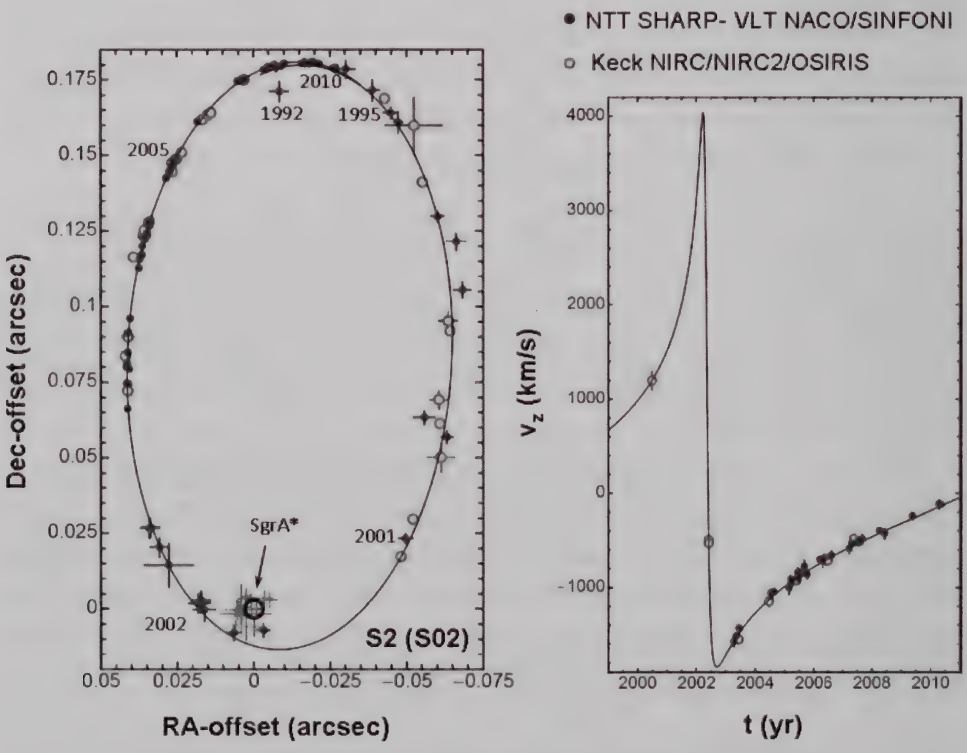

Figure 2. Orbit of star S2. The left side shows the orbit. The right side shows the radial velocity.

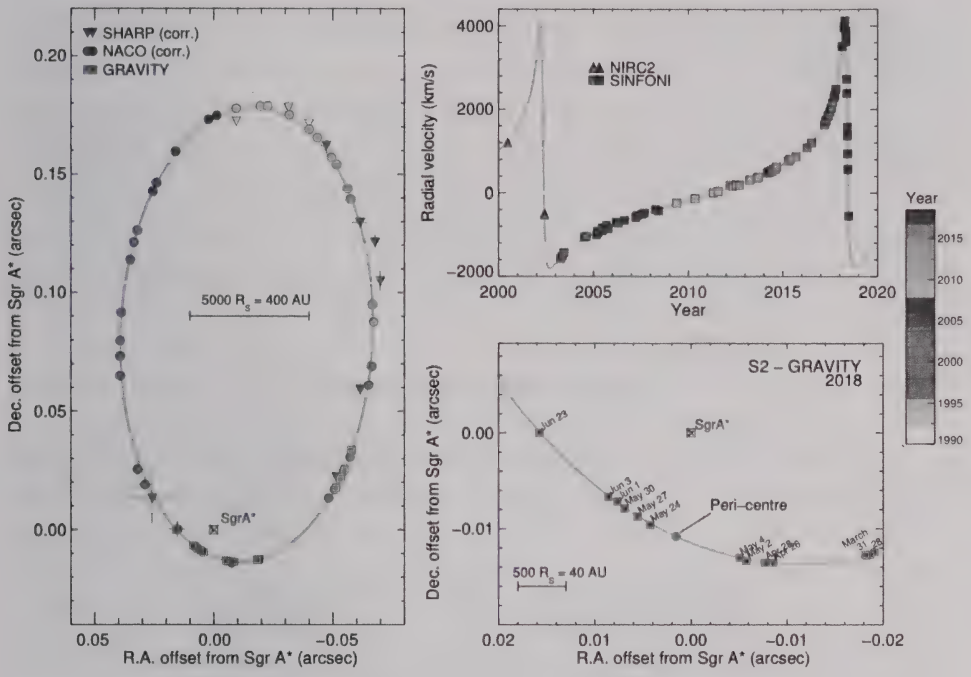

Figure 3. Summary of the observational results of monitoring the S2–Sgr A* orbit from 1992 to 2018.

In Figure 3, the panel on the left is the projected orbit of the star S2 on the sky (J2000) relative to the position of the compact radio source Sgr A* (brown crossed square at the origin). Triangles and circles (and 1σ uncertainties) denote the position measurements with SHARP at the Very Large Telescope, color-coded for time (color bar on the right side). The cyan curve shows the best-fitting S2 orbit to all these data, including the effects of general and special relativity. The bottom right panel shows a zoom-in around pericenter in 2018. The upper right panel shows the radial velocity of S2. S2 reached the pericenter of its orbit at the end of April 2002, and then again on 19 May 2018.

"Not only have the measurements provided exquisite kinematic evidence for a compact object in the Galactic centre, but also a sub-percent error estimate of the distance to the Galactic centre and a 20σ detection of the relativistic corrections needed to model the orbit of the star to the supermassive black hole. Furthermore, the team was able to detect the relativistic precession of the orbit—a truly remarkable experimental achievement addressing fundamental physics." (Nobel,

2020) The data predict a mass for the supermassive black hole of 4.3 million times the mass of the Sun.

We know that black holes can exist from the work of Penrose. From the two teams we know that there is a very compact object at Sgr A*. This object is not compatible with a dense cluster of stars but is compatible with a black hole. The Nobel Prize Committee awarded the 2020 Prize in physics to Roger Penrose and the two teams that studied Sgr A*.

Event Horizon Telescope

These data do not yet allow us to image the compact object at Sgr A* to no better than several hundred Schwarzschild radii. That means we cannot take an image of the supermassive black hole (which is invisible anyway). An as yet unattainable goal is to image the event horizon – one Schwarzschild radius from the center of the compact object. Yet astronomers used the Event Horizon Telescope (EHT) to see what is possible to see.

The EHT is an international collaboration that has formed to continue the steady long-term progress on imaging the event horizon. Very Long Baseline Interferometry (VLBI) at short wavelengths links radio dishes across the globe to create an Earth-sized interferometer. It has been used to measure the size of the emission regions of the two supermassive black holes with the largest apparent event horizons: Sgr A* at the center of the Milky Way; and M87 in the center of the Virgo A galaxy. In both cases the sizes match that of the predicted silhouette caused by the extreme lensing of light by the supermassive black holes.

The EHT array can be seen at https://bit.ly/3cultjY. All these EHT antennas act in unison to achieve an unprecedented angular resolution which could be comparable to reading a newspaper on the Moon from Earth.

The Silhouette

GTR predicts that light (photons) will bend around a nearby mass. It does not travel in Euclidean straight lines. GTR also predicts that photons emitted by the gas falling into a black hole should travel along

curved trajectories, forming a ring of light around a “shadow” corresponding to the location of the black hole. The term “shadow” isn't technically correct. What we hope to observe with the EHT is a “silhouette” of a black hole: its dark shape on a bright background of light coming from the surrounding matter, deformed by a strong space-time curvature. We still cannot see the invisible black hole. But we can hope to see the light surrounding it. The size and shape of this image can be predicted from the GTR equations. Size and shape depend mostly on black hole mass, and to a smaller degree, on its spin. GTR predicts a roughly circular shape of the shadow. Thus the shape of the shadow is a test of relativity. Figure 4 shows the image from the Event Horizon Telescope of Sgr A*. It is a three-dimensional shape which I cannot reproduce here. See the YouTube video that explains the three-dimensional shape seen for Sgr A* (YouTube, 2019).

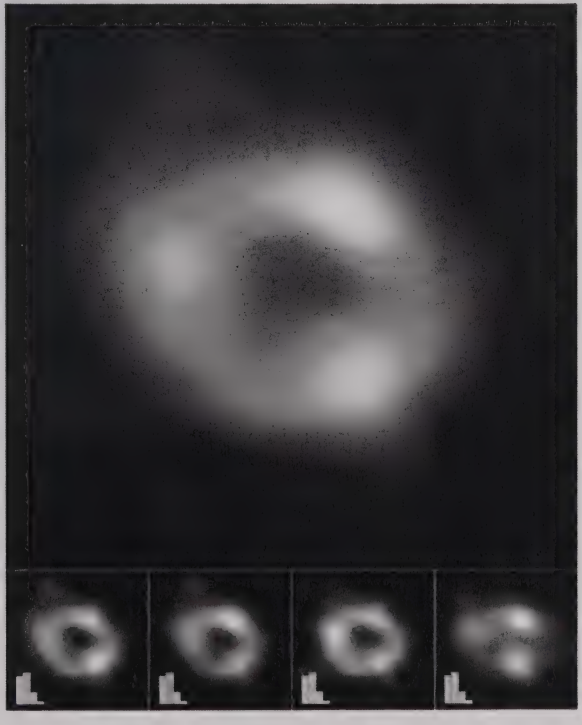

Figure 4. Image of Sgr A* taken with the Event Horizon Telescope

Black holes grow by eating up surrounding matter, but it's relatively difficult for matter to fall into a black hole. If matter isn't too close to the black hole and feels only gravity, it can orbit the black hole

indefinitely, the way the planets in our solar system orbit the Sun. Something more than gravity is needed to get the matter close enough to the black hole for the black hole to eat it. This process is called *accretion*, and it is driven by friction. **Accretion disks** form around black holes. An accretion disk is a swirling mass of gas and dust outside the Schwarzschild radius. Any matter that gets close enough to the Schwarzschild radius will form an accretion disk as it swirls into the black hole. As matter in the form of gas falls into the black hole, the gas loses gravitational energy and gets heated by friction. Friction causes different parts of the disk that slide by each other to lose energy and heat up, the same way heat is generated when you rub your hands together. The gas then forms a hot disk around the black hole and falls in, causing the black hole to grow. See Figure 5.

Figure 5. Accretion disk surrounding a black hole
with two plasma jets – courtesy NASA

Hot gas emits radiation we can observe (x-ray). Accretion disks emit bipolar plasma jets which emit radiation we can observe (radio). By looking in the radio regime for the jets and the x-ray regimes for the disks we can map out the jets and disk. These jets were observed long before

astronomers thought about black holes. Radio loud quasars were studied and not really understood until supermassive black holes were assumed to be in the centers of galaxies. Eventually astronomers built a list of suspected black holes. For these objects there were x-ray observations from a suspected accretion disk and radio observations of jets. The first star suspected to be a stellar mass black hole was the star Cygnus X-1.

Conclusion

After a short review of Newtonian physics we quickly move into Einstein's universe. The Schwarzschild metric is given and the concept of an event horizon that shields the insides from the rest of the universe defines cosmic censorship. The singularity that occurs when r goes to zero was debated for some time. Was it real or fiction? It took the discovery of quasars that drove astronomers to study the collapse of a star to $r = 0$. Roger Penrose then proved that once an event horizon had formed, it is impossible, within the general theory of relativity, and with a positive energy density, to prevent the collapse towards a singularity. So black holes were inevitable. No one had definitively found a black hole at this time but there were several candidates. Supermassive black holes were suspected to lurk at the centers of galaxies, especially quasars. Two teams began an expended set of observations of the center of the Milky Way, Sgr A*. Their results were conclusive – a compact, dense object compatible with a black hole sits at the Galactic center. The Nobel Prize Committee awarded the 2020 Prize in physics to Roger Penrose and the two teams that studied Sgr A*.

Bibliography

Howard, S. (2011). Black Holes Can Dance. Journal of the Washington Academy of Sciences, 97(2), 1-28.

Michell. J. (1784). On the Means of Discovering the Distance, Magnitude, &c. of the Fixed Stars, in Consequence of the Diminution of the Velocity of Their Light, in Case Such a Diminution Should be Found to Take Place in any of Them, and Such Other Data Should be Procured from Observations, as Would be Farther Necessary for That Purpose. By the Rev. John Michell, B. D. F. R. S. In a Letter to Henry Cavendish, Esq. F. R. S. and A. S. Philosophical Transactions of the Royal Society of London, 74, 35-57. Available at https://bit.ly/3ATPymp.

Miyoshi, M., Moran, J., Herrnstein, J., Greenhill, L., Nakai, N., Diamond, P., and Inoue, M. (1995). Evidence for a black hole from high rotation velocities in a sub-parsec region of NGC4258, Nature 373(6510), 127–129.

Montgomery, C., Orchiston, W., and Whittingham, I. (2009). Michell, Laplace and the origin of the black hole concept. Journal of Astronomical History and Heritage, 12(2), 90-96.

Nobel (2020). Press release: The Nobel Prize in Physics 2020. NobelPrize.org. Nobel Prize Outreach AB 2022. Sat. 27 Aug 2022. Available at https://bit.ly/3R8xoTy

Oppenheimer, J. R. and Snyder, H. (1939). On continued gravitational contraction, Physical Review, 56(5), 455–459.

Penrose, R. (1965). Gravitational collapse and space-time singularities, Physical Review Letters, 14(3), 57–59.

YouTube (2019) How to Understand the Black Hole Image. https://bit.ly/3ToepGk

Dr. Sethanne Howard is an astronomer retired from the US Naval Observatory as Chief of the Nautical Almanac Office. She worked at many places including Program Manager at the National Science Foundation for extragalactic astronomy and cosmology.

Annual Meeting

The Washington Academy of Sciences held its annual meeting on May 11, 2022.

Welcome Address

Lynnette Madsen

It is my privilege and great pleasure to welcome you to tonight's events. The Washington Academy of Sciences has a long legacy, and for more than a century after its inception, the Academy continues effectively to pursue its original goals, which include stimulating scientific interest and promoting science through collaboration, membership, publication, and dialogue. The Academy brings together scientists, encourages connections, particularly in the DC area, and with its strategic focus, encourages and creates an enabling environment for the next generation of scientists through its Junior Academy.

Many thanks to Vicky and the rest of the team for providing us with this lovely outdoor venue in Fairfax County. I also want to give a call out to the Program Planning Committee and the rest of the board for their diligent work to pull this event together tonight, thank you all. You will see a detailed agenda laid out – we will do our best to stick to this, please, so that we can end in good time on this weeknight.

Presidential Address

Ram D. Sriram (outgoing President)

Thank you all for attending today's event. As you all know the Washington Academy of Sciences is one of oldest scientific academies in the United States, going back to 1898. The founders included such luminaries as Alexander Graham Bell and Samuel Langley, secretary of Smithsonian Institution. The primary purpose of our academy is to encourage the advancement of science and to conduct endow, or assist investigation in any department of science." Several Nobel Laureates were members of our academy. Given the past history of our academy, I believe we should strive to keep up the reputation in advancing science. In my

presidential address last September, I brought up several issues to be addressed in 2022. Although, we did not have enough time to address all these, we did make some progress. There are several items I would like to bring to your attention.

Membership.

Our membership continues to increase, and we hope this trend continues. We also opened our membership to include other geographical areas, beside DMV (DC, Maryland, Virginia). We also looked into several tools that will aid in managing our membership. We would like you all to reach out to your colleagues regarding joining WAS.

Seminars.

We had several seminars from eminent scientists and engineers. These can be found on our website.

Junior academy.

The Academy has for many decades included a Junior Academy, which promotes STEM education in schools. We maintain a large list of judges for local science fairs. So far in 2022, our main event was judging of the STEM magnet program at Blair High School. These students are among the highest-achieving seniors in Montgomery County, Maryland. A team of 35 judges evaluated the advanced projects of 78 students. On February 16, Dr. Vijay Kowtha of IEEE and Paul Arveson, VP of the Junior Academy, handed out 24 trophies to the winners. We trust that this recognition will be helpful to the students in the future. We are proud to have had a small part in encouraging their careers and we anticipate many exciting discoveries that they are likely to make!

The Academy also supports work of mentors in after-school programs at the Air Tigers maker space in PG County and the Rockville Science Center. We hope to expand affiliations with more of these programs to bring professional scientists and young students together.

Journal.

Under the stewardship of Sethanne Howard, the Journal had a successful year. We had a special issue on ontologies, based on the yearly Ontology Summit. After decades of leadership, Sethanne decided to step down and Ken Baclawski has taken over as the editor of the journal. We deeply appreciate Sethanne's commintment and leadership, and we

welcome Ken as our new editor. Please encourage your colleagues to submit papers to the journal. Information about how to submit a paper can be found at the academy website.

Scientific advisory board.

We did not have the time to put together a scientific advisory board and we hope to set up a board this year.

By-Laws.

We have put in considerable work on amending our By-Laws and we hope to send a draft to our membership this summer.

Funding.

We had to negotiate a new contract with AAAS for her rental space. The costs have almost tripled. We are currently looking into additional fund raising and would appreciate any help from you all.

Finance Committee.

We have established a finance committee to look into the finances of WAS and balance our stock and bond portfolio. This will also help us in our yearly audit.

My thanks to the Board members for all their help so far. Our president-elect, Lynnette Madsen, along with her planning committee members, has done a marvelous job of organizing this banquet. Terry Longstreth with his knowledge-base of the academy made sure we followed proper procedures, and Mala Ramaiah took copious notes of the Board meetings throughout the year. Ron Hietala did a very diligent job as Treasurer. He will be stepping down after more than a decade of service. We greatly appreciate his dedication to the academy, and we will surely miss his expertise.

The entire award process was handled by Mahesh Mani, VP of Membership, and he was very diligent in ensuring that the process was rigorous and fair. We are very grateful to the External Awards Committee. Paul Arveson was responsible for setting up the webpage.

I believe the academy will be in excellent hands under the leadership of Lynnette Madsen, who will provide her remarks at the end of the awards presentation.

The Committee of Tellers have the following to report regarding the outcome of ballot counting.

President: Lynnette Madsen

President-Elect: Mahesh Mani

Secretary: Mala Ramaiah

Treasurer: David Torain

VP Administrative Affairs: Terry Longstreth

VP Affiliated Societies: Parisa Meisami

VP Membership: David Torain (who will take over as the Treasurer)

VP Junior Academy: Paul Arveson

Journal Editor (Ex Officio): Kenneth Baclawski

Members at Large: Mei Sun, Anne Kornahrens, Judy Stavely, Mina Izadjoo

Delegates: Michael Cohen, Jorome (Jerry) Gibbon

Immediate Past President (Ex Officio): Ram D. Sriram

Wrap-Up Address

Lynnette Madsen (incoming President)

It is my privilege and great pleasure to take on my next role for Washington Academy of Sciences at the end of this Banquet.

I commend Ram for excellent job at being President of the Academy. Ram has initiated some wonderful updates and advances for the Washington Academy of Sciences. One of these is an update to the **bylaws**; this is urgently needed to modernize and streamline our processes - I trust that this will be completed shortly. Concomitant with this are discussions to implement **electronic processes** to revamp what may be viewed as cumbersome and dated procedures **for joining, renewing and paying** for membership. However, I hasten to stress that we will retain printed mail processes for members who prefer them. A task force has been exploring the best **financial arrangements** to underpin the academy; we will move ahead with their recommendations. Finally, I will ask the board to complete

the work to give **Fellows greater prominence** within the Academy. (4 items)

Paramount to continued success is to increase engagement of members and expand activities to support and promote great science, and I will ask the board to brainstorm on these challenges during this year to move the Academy forward. There are several aspects to this undertaking. First, I will ask the board will conduct a strengths-weaknesses-opportunities-threats or **SWOT analysis**. Next, we will **define potential projects and prioritize them**. Throughout we will be seeking input from the membership, which is expanding especially beyond the DMV region.

Finally, I would like to see new faces take a few of the six slots of Members-at-Large on the Board; this is a great entry point to our board. To free up slots, where appropriate, some existing board members may transition to Affiliate Representative roles on the Board. In this vein, we will be refining our **transition processes including on-boarding** of new board members.

In closing, I encourage you to reach out to me or the new President-Elect, Mahesh, and express your interest in becoming more involved in an activity, on a committee, or with the board.

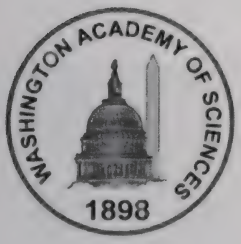

Washington Academy of Sciences
2022 Awardees
Congratulations

2022 Award Recipients

All awards were given at the WAS annual banquet and awards ceremony on May 11th, 2022 (https://www.washacadsci.org)

Krupsaw Award for Non-Traditional Teaching: Ivan Galysh

Distinguished Career Award in Biochemistry: Dr. Seymour Garte

Distinguished Career Award in Chemistry: Dr. Edwin J. Heilweil

Distinguished Career Award in Computer Science and Policy: Dr. Sethuraman Panchanathan

Distinguished Career Award in Engineering: Dr. John L. Anderson

Excellence in Research Award in Applied Mathematics: Dr. Paul Patrone

Excellence in Research Award in Chemical Engineering: Dr. Jiann Yang

Excellence in Research Award in Physical and Information Sciences: Dr. Alexey Gorshkov

Leadership Award for Contributions to Field of Forensic Science: Barbara Guttman

Leadership Award for Developing Science and Engineering Policy: Dr. Guru Madhavan

Leadership Award in Manufacturing Engineering: Dr. Kevin Jurrens

The WAS Distinguished Service Award (Treasurer): Dr. Ronald Heitala

The WAS Distinguished Service Award (Journal Editor): Dr. Sethanne Howard

Krupsaw Award for Non-Traditional Teaching

Ivan Galysh

Ivan Galysh (left) received the Krupsaw Award, here presented by Dr. Vijayanand Kowtha (right) (photo by Judy Staveley).

Galysh has spent hundreds of hours each year providing direct hands-on instruction, supervision, and motivation to multiple teams of students in grades seven through 12. Ivan organizes and runs the CanSat Competition—a competition created to provide a unique opportunity for teams to design and build a satellite that fits inside a soda can. Held annually in Texas, the CanSat rocket launch involves student teams from around the world and is sponsored by aerospace industries, associations, and NRL. He is also founder of the national Battle of the Rockets competition developed for high school and university student teams that involves the design and launch of rover-type payloads on large rockets.

Distinguished Career Award in Biochemistry

Seymour Garte

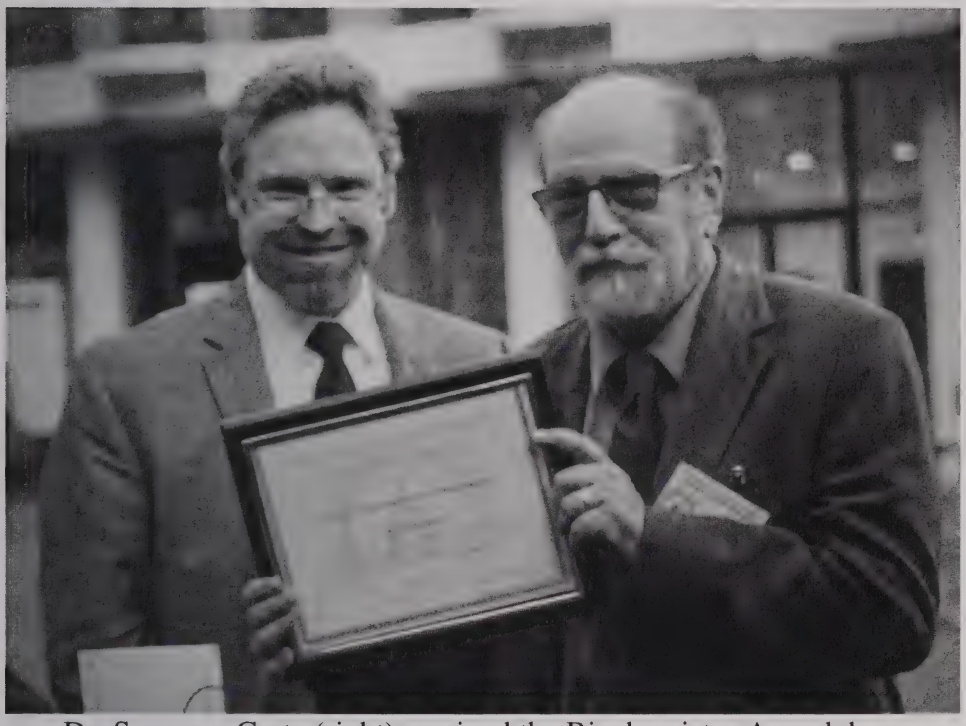

Dr. Seymour Garte (right) received the Biochemistry Award, here presented by Mike Beidler (left) (photo by Judy Staveley).

Seymour (Sy) Garte has been a tenured professor at New York University, Rutgers University, and the University of Pittsburgh, division director at the Center for Scientific Review of the National Institutes of Health, and interim vice president for research at the Uniformed Services University of the Health Sciences. He is currently visiting professor of pharmacology and toxicology at Rutgers University.

Distinguished Career Award in Chemistry

Edwin J. Heilweil

Dr. Edwin J. Heilweil (left) received the Chemistry Award, here presented by Dr. Jerry Fraser (right) (photo by Judy Staveley).

Heilweil began his career at NIST/NBS as a National Research Council Postdoctoral Fellow in 1983. He received several awards including the Instrument Society of America Beckman Award (1989), Department of Commerce Stratton Award (1991), and Sigma Xi Young Scientist Award (1992). In 2008 he received the NIST/DoC Silver Medal for "contributions to ultrafast optical studies of vibrational energy transfer and terahertz spectroscopy." He was recognized by receiving the Lifetime Achievement award from the TRVS community in 2017 for which a Special Issue in the journal Chemical Physics was issued on his behalf in 2018. Heilweil also received a NIST/DoC Bronze Medal for work on Ultrafast Pulsed Laser Safety Eyewear in 2018.

Distinguished Career Award in Computer Science and Policy

Sethuraman Panchanathan

Dr. Sethuraman Panchanathan (left) received the Policy Award, here presented by Dr. Kumara Soundar (right) (photo by Judy Staveley).

Sethuraman is the Director of the National Science Foundation, a post he has held since June 2020. He previously served as the Executive Vice President, ASU Knowledge Enterprise Development and Chief Research and Innovation Officer at Arizona State University (ASU). He was also Director of the Center for Cognitive Ubiquitous Computing, Foundation Chair of Computing and Informatics at ASU and Professor in the School of Computing, Informatics, and Decision Systems Engineering part of the Ira A. Fulton Schools of Engineering.

Distinguished Career Award in Engineering

John L. Anderson

Dr. John L. Anderson (left) received the Engineering Award, here presented by Dr. Guru Madhavan (right) (photo by Judy Staveley).

John is the current President of the National Academy of Engineering. He served as the eighth president of Illinois Institute of Technology (IIT). Prior to his appointment at IIT, Anderson held positions in academia at various institutions, serving both as the provost of Case Western Reserve University and the dean of the College of Engineering at Carnegie Mellon University. He was elected to the National Academy of Engineering in 1992 for contributions to the understanding of colloidal hydrodynamics and membrane transport phenomena.

Excellence in Research Award in Applied Mathematics

Paul Patrone

Dr. Paul Patrone received the Applied Mathematics Award. Dr. Ronald Boisvert (left) accepted the award on behalf of Dr. Patrone, here presented by Dr. Mahesh Mani (right) (photo by Judy Staveley).

Paul Patrone has been a staff member in the Applied and Computational Mathematics Division at NIST since 2015, His physical insight and prodigious analytic skills have enabled him to make extraordinary advances in material science, engineering, physics, and biotechnology, which have had broad impact. Among his many accomplishments, he developed a new method of baseline subtraction for analyzing qPCR data that results in measurements that are 10 times more sensitive than before. A large Arizona-based testing lab which adopted his procedure has greatly reduced its false negatives as a result, thus helping to significantly reduce COVID-19 transmission.

Excellence in Research Award in Chemical Engineering

Jiann Yang

Dr. Jiann Yang (left) received the Chemical Engineering Award, here presented by Dr. Joannie Chin (right) (photo by Judy Staveley).

Jiann Yang is the Deputy Chief of the Fire Research Division at NIST. The Division develops and utilizes measurement science to enhance the disaster resilience of buildings and wildland-urban interface communities, improve fire fighter safety and effectiveness, and enable performance based design through cost-effective engineered fire safety for people, products, structures, and communities. He has conducted research on fire dynamics and suppression, halon replacements, droplets and sprays, aerosol dynamics, micro-gravity combustion, two-phase flows, hydrogen fire safety, greenhouse gas emission measurements, and transportation fire safety. He was awarded the U.S. Department of Commence Bronze Medal in 2000, Gold Medal in 2005, and the SAE International Arch T. Colwell Merit Award in 2008. He is a Fellow of the American Society of Mechanical Engineers.

Excellence in Research Award in Physical and Information Sciences

Alexey Gorshkov

Dr. Alexey Gorshkov (left) received the Award, here presented by Nobel Laureate Dr. William Phillips (right) (photo by Judy Staveley).

Alexey Gorshkov is a fellow of the Joint Quantum Institute and Joint Center for Quantum Information and Computer Science, a partnership of the University of Maryland and NIST.

Leadership Award for Contributions to Field of Forensic Science

Barbara Guttman

Barbara Guttman (left) received the Forensic Science Award, here presented by Dr. Ram Sriram (right) (photo by Judy Staveley).

Barbara Guttman is the leader of the Software Quality Group, where she leads projects in computer forensics and software assurance. She has been awarded the U.S. Department of Commerce Gold Medal in 2008 for work developing guidelines for voting systems and the NIST Bronze Medal in 1995 for work in computer security.

Leadership Award for Developing Science and Engineering Policy

Guru Madhavan

Dr. Guru Madhavan (left) received the Policy Award, here presented by Dr. Ram Sriram (right) (photo by Judy Staveley).

Guru Madhavan is the Norman R. Augustine Senior Scholar and senior director of programs at the U.S. National Academy of Engineering. He is a biomedical engineer and senior policy adviser. He has been named a distinguished young scientist by the World Economic Forum.

Leadership Award in Manufacturing Engineering

Kevin Jurrens

Dr. Kevin Jurrens (left) received the Manufacturing Engineering Award, here presented by Al Wavering (right) (photo by Judy Staveley).

Kevin Jurrens is the Deputy Chief of the Intelligent Systems Division (ISD) in the Engineering Laboratory (EL) of the National Institute of Standards and Technology (NIST). Kevin has been involved in rapid prototyping and additive manufacturing since the mid-1990s, contributing to both the 1998 and 2009 industry roadmaps. Kevin has contributed to machining process metrology and modeling, standardized data representations for machine tool and cutting tool information, reverse engineering technologies for component repair and replacement, and development of the international STEP (ISO 10303) standard for product definition data. He currently serves on the Executive Committee for the ASTM F42 standards committee on Additive Manufacturing Technologies and as the NIST representative for both the National Additive Manufacturing Innovation Institute (NAMII) and the Additive Manufacturing Consortium (AMC).

The WAS Distinguished Service Award (Treasurer)

Ronald Hietala

Dr. Ronald Heitala (right) received the Service Award, here presented by Ram D. Sriram (left) (photo by Judy Staveley).

Ronald O. Hietala prepared for life by earning a Master of Science degree from Hollins College in Virgina and a PhD degree from the University of Tennessee in Knoxville, both in psychology. His major area of study was industrial psychology and one of his main interests was statistics. To this day, he finds it regrettable that so few people are taught much practical statistics. He worked in personnel research at the U.S. Internal Revenue Service three years and for five years at the Department of Housing and Urban Development. Then, for 14 years, he worked at the U.S. Mint, where he made a gradual change from personnel research into training and development, which he found much more satisfying. After 22 years, seeking a change, he left the federal government and worked in private tech-related industry as a contracting officer, which he also found very satisfying. He is now almost fully retired, but his interests continue to evolve. He is beginning work on a book about the Kensington rune stone, which he regards as a fascinating mystery of U.S history.

The WAS Distinguished Service Award (Journal Editor)

Sethanne Howard

Dr. Sethanne Howard (right) received the Service Award, here presented by Ram D. Sriram (left) (photo by Judy Staveley).

Sethanne Howard has a PhD in astrophysics. She worked as an oceanographer, meteorologist, astronomer, and Chief of the Nautical Almanac Office. She was the Program Manager for Extragalactic Astronomy and Cosmology at the National Science Foundation; now retired. Her avocation is the history of women in science and technology. She represents the American Astronomical Society on the board of the Academy.

Washington Academy of Sciences Board of Managers 2022-2023

From left: Paul Arveson, Terry Longstreth, Mahesh Mani, Parisa Meisami, Ram D. Sriram, Judy Staveley, Michael Cohen, Sethanne Howard, Lynnette Madsen, Mina Izadjoo, Mala Ramaiah, Mei Sun, Ron Hietala, Joanne Horn (photo by Judy Staveley). Not shown: David Torain, Lisa Frehill, Anne Kornahrens, Kenneth Baclawski

James John Filliben

Washington Academy of Sciences Fellow James Filliben unexpectedly passed away on August 15, 2022. Jim earned his Ph.D. in statistics at Princeton University in 1969 with John Tukey as his dissertation advisor. His 53-year career was at the National Institute of Standards and Technology (NIST), where was a Senior Mathematical Statistician. In 2021, he was named Dean of Staff, given to NIST's longest-tenured technical staff member. His illustrious career includes contributions in scientific and statistical problem formulation, experiment design, exploratory data analysis and statistical graphing. In 1978, he developed Dataplot, an innovative statistical software package still in use today. He worked on effective randomization techniques for draft lotteries, the effects of Daylight Savings Time and the collapse of the World Trade Center, and was prolific in the number of talks given and scholarly papers written. He delighted in mentoring new colleagues and doctoral students. For his many accomplishments, Jim was named a Fellow of both the Washington Academy of Sciences and the American Statistical Association, and earned multiple Gold, Silver and Bronze Medals from the Department of Commerce. Dr. Filliben was recognized for his significant, life-long contributions to physical science, engineering, and metrological research using sound statistical methods for design of experiments and data analysis. Full Obituary: https://bit.ly/3AuBIW1

Dr. James Fillben (left) received the Award for Distinguished Career in Science in 2017, here presented by Dr. Chuck Romine (photo by Ram Sriram).

Delegates to the Washington Academy of Sciences Representing Affiliated Scientific Societies

Acoustical Society of America	Paul Arveson
American/International Association of Dental Research	J. Terrell Hoffeld
American Association of Physics Teachers, Chesapeake Section	Frank R. Haig, S. J.
American Astronomical Society	Sethanne Howard
American Fisheries Society	Lee Benaka
American Institute of Aeronautics and Astronautics	David W. Brandt
American Institute of Mining, Metallurgy & Exploration	E. Lee Bray
American Meteorological Society	Vacant
American Nuclear Society	Charles Martin
American Phytopathological Society	Vacant
American Society for Cybernetics	Stuart Umpleby
American Society for Microbiology	Vacant
American Society of Civil Engineers	Vacant
American Society of Mechanical Engineers	Daniel J. Vavrick
American Society of Plant Physiology	Mark Holland
Anthropological Society of Washington	Vacant
ASM International	Toni Marechaux
Association for Women in Science	Jodi Wesemann
Association for Computing Machinery	Vacant
Association for Science, Technology, and Innovation	F. Douglas Witherspoon
Association of Information Technology Professionals	Vacant
Biological Society of Washington	Vacant
Botanical Society of Washington	Chris Puttock
Capital Area Food Protection Association	Keith Lempel
Chemical Society of Washington	Vacant
District of Columbia Institute of Chemists	Vacant
Eastern Sociological Society	Ronald W. Mandersheid
Electrochemical Society	Vacant
Entomological Society of Washington	Vacant
Geological Society of Washington	Jeff Plescia Jurate Landwehr
Historical Society of Washington DC	Vacant
Human Factors and Ergonomics Society	Gerald Krueger

(continued on next page)

Delegates to the Washington Academy of Sciences Representing Affiliated Scientific Societies

(continued from previous page)

Institute of Electrical and Electronics Engineers, Washington Section	Richard Hill
Institute of Food Technologies, Washington DC Section	Taylor Wallace
Institute of Industrial Engineers, National Capital Chapter	Neal F. Schmeidler
International Association for Dental Research, American Section	Christopher Fox
International Society for the Systems Sciences	Vacant
International Society of Automation, Baltimore Washington Section	Richard Sommerfield
Instrument Society of America	Hank Hegner
Marine Technology Society	Jake Sobin
Maryland Native Plant Society	Vacant
Mathematical Association of America, Maryland-District of Columbia-Virginia Section	John Hamman
Medical Society of the District of Columbia	Julian Craig
National Capital Area Skeptics	Vacant
National Capital Astronomers	Jay H. Miller
National Geographic Society	Vacant
Optical Society of America, National Capital Section	Jim Heaney
Pest Science Society of America	Vacant
Philosophical Society of Washington	Michael P. Cohen
Society for Experimental Biology and Medicine	Vacant
Society of American Foresters, National Capital Society	Marilyn Buford
Society of American Military Engineers, Washington DC Post	Vacant
Society of Manufacturing Engineers, Washington DC Chapter	Vacant
Society of Mining, Metallurgy, and Exploration, Inc., Washington DC Section	E. Lee Bray
Soil and Water Conservation Society, National Capital Chapter	Erika Larsen
Technology Transfer Society, Washington Area Chapter	Richard Leshuk
Virginia Native Plant Society, Potomac Chapter	Alan Ford
Washington DC Chapter of the Institute for Operations Research and the Management Sciences (WINFORMS)	Meagan Pitluck-Schmitt
Washington Evolutionary Systems Society	Vacant
Washington History of Science Club	Albert G. Gluckman
Washington Paint Technology Group	Vacant
Washington Society of Engineers	Alvin Reiner
Washington Society for the History of Medicine	Alain Touwaide
Washington Statistical Society	Michael P. Cohen
World Future Society, National Capital Region Chapter	Jim Honig

Washington Academy of Sciences
Room 455
1200 New York Ave. NW
Washington, DC 20005
Return Postage Guaranteed